227 (2023) 211936

Contents lists available at ScienceDirect

Geoenergy Science and Engineering

journal homepage: www.sciencedirect.com/journal/geoenergy-science-and-engineering

A critical review on low salinity waterflooding for enhanced oil recovery: Experimental studies, simulations, and field applications

Grant Charles Mwakipunda [a], Rui Jia [b], Melckzedeck Michael Mgimba [a,c], Mbega Ramadhani Ngata [a], Athumani Omari Mmbuji [a,d], Annasi Ayubu Said [e], Long Yu [a,*]

[a] Key Laboratory of Theory and Technology of Petroleum Exploration and Development in Hubei Province, China University of Geosciences, Wuhan, 430074, China
[b] School of Geosciences, Yangtze University, China
[c] Mbeya University of Science and Technology (MUST), P.O Box 131, Mbeya, Tanzania
[d] Arusha Technical College, P. O. Box 296, Arusha, Tanzania
[e] Department of Physics, School of Mathematics and Physics, China University of Geosciences, Wuhan, 430074, China

A R T I C L E I N F O

Keywords:
Enhanced oil recovery
Low salinity waterflooding
Residual oil saturation
Formation damage
Energy

A B S T R A C T

Due to the challenges of discovering new energy sources, enhanced oil recovery (EOR) techniques remain a potential area of research interest to produce residual oil in matured reservoirs after the depletion of primary and secondary recovery energy. Low salinity waterflooding (LSWF) is one of the promising research areas of interest in EOR techniques for the micro sweep efficiency of residual oil saturation. This review paper critically analyzed LSWF potentiality for exploiting residual oil in matured reservoirs. The results revealed that, despite various researchers' findings from developed theories, experimental data, modeling and simulations, single well chemical tracer tests (SWCTT), and pilot tests, there are limited studies that analyzed and addressed in detail the field application of LSWF due to unclear mechanisms, inconsistency research findings, and failure on SWCTT and pilot tests. Further, this paper describes LSWF's activities that led to the success of LSWF field application in the Pervomaiskoye oil field in Russia and Clair ridge in the United Kingdom (UK) towards entire field operations after the first oil production in 2018. Furthermore, the study showed that the formation damage has positively impacted oil recovery by mobilizing residual oil in unswept areas. The identified research gaps, such as dominant mechanism on LSWF, modeling and simulations of fluid-fluid interactions effects, osmotic effects contributions on LSWF, etc., and findings of this paper shall help different researchers and shareholders to conduct more research to meet global energy for the future demands. The challenges which need to be considered towards successfully full field LSWF operations includes reservoir heterogeneity problems, scaling problem, clay swelling, quality of injected water, cost of the projects, salt dispersion and brine mixing, health and safety issues, environmental issues, etc. On the contrary, from laboratory studies, few simulation studies, and few pilot field applications, hybrid LSWF has shown a great potential to increase oil recovery over LSWF. However, due to additional cost of chemicals could make a hybrid LSWF challenging economically in the full field application.

1. Introduction

More than 50% of oil remains in the reservoir after primary and secondary recovery energy depletion (Afifi et al., 2021; Akbarifard et al., 2020; Deng et al., 2021; Ghasemi and Shafiei, 2022; Hussain et al., 2022). Conventional waterflooding is the main secondary oil recovery method applied in several matured oil fields to increase oil recovery (Agzamov et al., 2023; Willhite, 1986). However, low salinity waterflooding (LSWF) has recently gained more attention as an alternative to conventional waterflooding and other tertiary recovery techniques because of its lower cost, environmentally friendly, and high oil recovery (Aljaberi and Sohrabi, 2019; Farzaneh et al., 2017; Lager et al., 2008d; Sagbana et al., 2022). Laboratory core flooding has confirmed that LSWF increases the oil recovery factor from 2% to 40% over conventional waterflooding for both secondary and tertiary recoveries (Hisham Ben et al., 2019), depending on both rock-fluid and fluid-fluid interactions (Dordzie and Dejam, 2022; Farhadi et al., 2021; Fattahi Mehraban et al., 2020; Gbadamosi et al., 2022; Lager et al., 2008c;

* Corresponding author.
E-mail address: yulong36@cug.edu.cn (L. Yu).

https://doi.org/10.1016/j.geoen.2023.211936
Received 13 February 2023; Received in revised form 18 May 2023; Accepted 20 May 2023
Available online 22 May 2023

McGuire et al., 2005a). In addition, LSWF is superior over other enhanced oil recovery (EOR) techniques since it can be combined with other EOR techniques to form hybrid LSWF such as carbon dioxide-LSWF (CO_2-LSWF), surfactants-LSWF, alkali-LSWF, polymer-LSWF, low salinity steam flooding, etc., In Alaska oil field, injected low salinity brine with less than 5000 ppm improved the oil recovery factor by 6–12% of original oil in place (OOIP) (Chowdhury et al., 2022; Janssen et al., 2020; Lager et al., 2008a; McGuire et al., 2005a). Furthermore, Alhuraishawy et al. (2018) reported that as salinity concentration decreased, the oil recovery factor (RF) increased; for instance, 1 wt%,0.1 wt%, and 0.01 wt of NaCl resulted in oil recovery factor of 45%, 60%, and 70%, respectively. Table A1 in appendix A summarizes the effects of LSWF in reducing residual oil saturation in different formations.

However, the main challenge of LSWF is its underlying mechanisms, which are not well verified and are continuously debated. Different researchers come with inconsistent results, which raises more shareholders to continue researching using advanced tools (Mahani et al., 2015, 2016; Nasralla et al., 2013). Then, it is still a challenge to determine the process behind LSWF mechanisms for various oil fields, especially for carbonate reservoirs (Javadi and Fatemi, 2022; Lyu et al., 2022). It is reported that the linkage mechanisms for wettability alteration induced by LSWF are fluid-to-fluid (Ayirala et al., 2018a, 2018b; Liu et al., 2021; Mahmoudzadeh et al., 2022; Mehraban et al., 2022) and rock-fluid (Bhicajee and Romero-Zerón, 2021; Mehana et al., 2020; Shabani and Zivar, 2020; Xie et al., 2019). These processes are triggered by multi-ion exchange (Bhicajee and Romero-Zerón, 2021; Shabani and Zivar, 2020), clay hydration and fines migration(Al-Sarihi et al., 2018; Nguyen et al., 2020), electric double-layer expansion(Mehana et al., 2020; Pourakaberian et al., 2021; Xie et al., 2019), pH increase(Austad et al., 2010a; McGuire et al., 2005a), mineral dissolution (Pu et al., 2010), osmotic water transport (Fang et al., 2020; Fredriksen et al., 2017a; Sandengen et al., 2016; Takeda et al., 2021; Yan et al., 2020), viscoelasticity increase (Ayirala et al., 2018a, 2018b), salting effect (Al-Shalabi and Sepehrnoori, 2016; RezaeiDoust et al., 2009), etc., However, these mechanisms have not been widely accepted and approved for adoption for field application(Aljaberi et al., 2022b). All these mechanisms play a significant role in rock wettability changes from oil-wet to mixed wet or water wet. This wettability alteration helps to increase microscopic sweep efficiency, thus improving oil recovery. Previous researchers have presented their results from core flooding experiments, modeling and simulations, and field applications of LSWF on enhancing oil recovery. Their findings contradict to each other, which mechanism is behind wettability alteration.

Many researchers have found that rock-fluid interaction contributes to wettability alteration (Al-Shalabi and Sepehrnoori, 2016; Austad et al., 2010b; McGuire et al., 2005b; Mehana et al., 2020; Nguyen et al., 2020; Pourakaberian et al., 2021; RezaeiDoust et al., 2009; Shabani and Zivar, 2020; Xie et al., 2019). However, it has recently been found that wettability alteration is due to fluid-fluid interactions, not rock-fluid interactions, as suggested earlier after several micromodel experiments (Ayirala et al., 2018a, 2018b; Bidhendi et al., 2018; Emadi and Sohrabi, 2013; Liu et al., 2021; Mahmoudzadeh et al., 2022; Mehraban et al., 2022; Sandengen et al., 2016). Hence, this study reviewed the LSWF as one of the ongoing research areas on enhancing oil recovery from the matured oil reservoir, emphasizing LSWF mechanisms, experimental works, modeling and simulations, and field applications. The results, setbacks, and on-going challenges and limitations herein are expected to motivate stakeholders, academicians, and researchers to adequately progress into farther research associated with LSWF applications on enhancing oil recovery and their economic entanglements to meet future global energy demand. Furthermore, this study has discussed the experimental investigation of formation damage effects during LSWF on the micromodel scale due to clay-induced fluid flow diversion and clay swelling and migration mechanisms based on brine content and compositions, which has never been addressed in previously published reviews. In addition, this review, for the first time, discussed in detail modeling and simulation with governing equations during LSWF. This review paper is divided into several sections: introduction, LSWF mechanisms, experimental parts, modeling and simulation of LSWF, hybrid LSWF, LSWF field applications, formation damage effects during LSWF, challenges encountered during LSWF, research gaps and future works, finalized by conclusions and recommendations.

1.1. Screening conditions for LSWF

After several experiments done by researchers, there are necessary conditions to be met for LSWF to take place. Porous medium, which includes sandstone and carbonates formations. It has been found that LSWF improved oil recovery in both sandstones, as delineated by (Lager et al., 2008a, 2008b; Pu et al., 2008; RezaeiDoust et al., 2009; Zhang and Morrow, 2006), and carbonates, as observed by (Al-Harrasi et al., 2012; Alhammadi et al., 2017; Derkani et al., 2018; Ding et al., 2019, 2020; Farhadi et al., 2022; Lashkarbolooki et al., 2016; Nasralla et al., 2015; Sohal et al., 2017; Tetteh and Barati, 2018; Webb et al., 2005; Xiao et al., 2018; Yousef et al., 2012; Zhang and Sarma, 2012). Also, clay content (7–30%) plays a significant role in wettability change (Rotondi et al., 2014a). Another is oil polarity; oil contains acids and bases (polar components) that influence LSWF because it has been observed that LSWF did not occur in refined oil (Torrijos et al., 2018). Else is formation water (brine) having divalent cations (Ca^{2+} and Mg^{2+}). The efficiency of LSWF depends on the initial formation water saturation (Austad et al., 2010a; Mirchi et al., 2017; Tang and Morrow, 1999a). Farther is low salinity injection water, having salinity from 1000 ppm to 2000 ppm, sensitive to (Ca^{2+} vs. Na^{+}) ionic composition. However, salinity effects have been observed up to 5000 ppm. In addition, the salinity of injected water below 5000 ppm and above critical flocculation concentration (CFC) to prevent clay swelling and formation damage is essential (McGuire et al., 2005a) (Austad et al., 2010a; Tang and Morrow, 1999a).

Furthermore is temperature; in all laboratory experiments of LSWF, there is no reported range of temperature to conduct experiments even though most successive experiments were conducted at room temperature and below 100 °C (Austad et al., 2010a) for sandstones and above 100 °C for some carbonates experiments (RezaeiDoust et al., 2009). Also, produced water; is important to measure the formation water pH and should be less than 7, which usually rises after low salinity injection and helps in determining the salinity water to be injected (Austad et al., 2010a; Lager et al., 2008a; Rotondi et al., 2014a). Another is high residual oil saturation.The screening criteria are summarized in Table 1.

1.2. Working flow for LSWF

Several steps must be followed for LSWF to come into large-scale field applications to avoid uncertainties and economic loss. According to Eni's experience, which started doing research in 2006, the steps to be followed are shown in Fig. 1. The first step involves EOR screening,

Table 1
Petrophysics and fluid properties screening criteria for LSWF.

Parameter	Value	Units
Clay content	7–30	%
The salinity of injected water	<5000 for sandstones and <10000 for carbonates	ppm
Temperature	Room temperature to 100 for sandstones and >100 for some carbonates	°C
Porosity	10–30	%
Oil density (API)	12–39	API
pH of formation water	<7	–
High residual saturation	>50	%
Permeability	0.25–4800	mD
pH of oil	6.9–10.5	–
Viscosity (oil)	0.52–112	cP

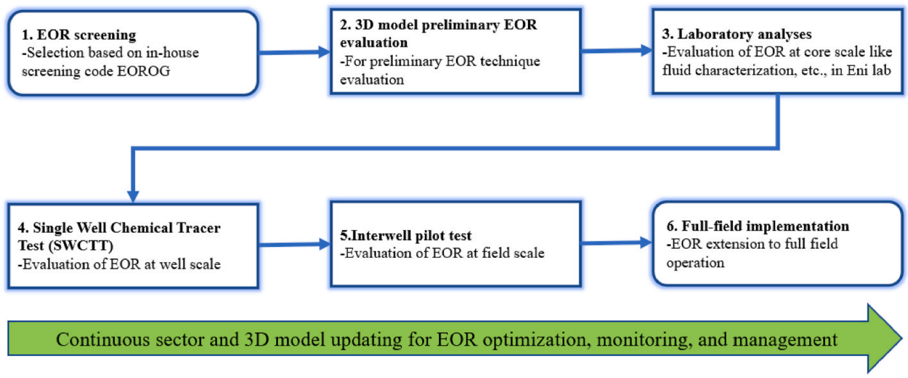

Fig. 1. Flowchart for LSWF (Rotondi et al., 2014b).

which involves selecting a field suitable for LSWF, as summarized in section 1.1. In this step, feasibility and operational evaluation should be conducted based on the environments and the required resources. The second step is the 3D model preliminary EOR evaluation which involves estimating the amount of oil that can be recovered after LSWF application. The third step is laboratory analysis involving core flooding experiments under reservoir conditions, fluid characterization, and formation evaluation for LSWF using different laboratory apparatuses. Also, in this step, basic mechanisms like rock-fluid or fluid-fluid interactions in increasing oil recovery are evaluated. After comprehending it on the laboratory scale, investors are more confident implementing it on the field scale. The fourth step is the single-well chemical tracer test (SWCTT), which measures near-well LSWF efficiency. A tracer tool measures a well residual oil saturation from a 5–6 m radius. The fifth step is the interwell test; this depends on the laboratory and SWCTT effectiveness results. The last step is evaluating full field implementation, which involves designing and building a desalination unit, field installation facilities, and economic analysis. Throughout the workflow, several modeling and simulation by using commercial reservoirs simulators such as CMG (GEM/STARS), UTCHEM-IPHREEQC, and Schlumberger ECLIPSE are conducted to predict future performance, which will help in the decision-making process. Pilot tests and monitoring of LSWF must be well executed to avoid uncertainties (Rotondi et al., 2014b).

1.3. Low salinity waterflooding mechanisms evolution

Wettability alteration from oil-wet to either mixed wet or water wet is believed to be the main process during LSWF for increasing oil recovery (Anderson, 1986; Morrow, 1990; Morrow et al., 1998a). However, the dominant mechanisms behind the wettability alteration are not clear. Several low-salinity waterflooding mechanisms were established from conducted laboratory experiments for wettability alteration. These are fines migration(Bedrikovetsky et al., 2015; Morrow et al., 1998b; Nguyen et al., 2020; Tang and Morrow, 1999a; Zeinijahromi et al., 2016); pH increase effects (Austad et al., 2010a; Ma and James, 2022); mineral dissolution(Austad et al., 2010a; McGuire et al., 2005a); emulsification (Morishita et al., 2020; Tang and Morrow, 1999b); interfacial tension reduction(Austad et al., 2010a), multicomponent ion exchange (MIE) (Hien et al., 2021; Pouryousefy et al., 2016; Sharma and Filoco, 2000; Tang and Morrow, 1999b; Zhang and Morrow, 2006), electric double layer expansion(Anderson, 1986; Katende and Sagala, 2019; Morrow, 1990; Morrow et al., 1998a; Nasralla and Nasr-El-Din, 2014; Sheng, 2014). These mechanisms are explained based on the formation type in the next section. The discovery timeline for wettability change during LSWF mechanisms is summarized in Fig. 2.

2. Low salinity waterflooding mechanisms

As previously divulged, LSWF mechanisms are either due to rock-fluid or fluid-fluid interactions or rock-fluid-fluid interaction (in carbonate reservoirs), commonly known as crude oil-brine-rock (COBR) interaction; this section discusses these interactions believed to influence LSWF mechanisms on increasing oil recovery.

2.1. Rock-fluid LSWF

2.1.1. Fines migration

It was the first proposed LSWF mechanism by Tang and Morrow (1999b). After smart water injection into the formation, clay becomes negatively charged due to brine-clay interactions. These negative charges cause repulsive forces development in the formation, resulting in clay migrations after detachment. These clay migration damage pore

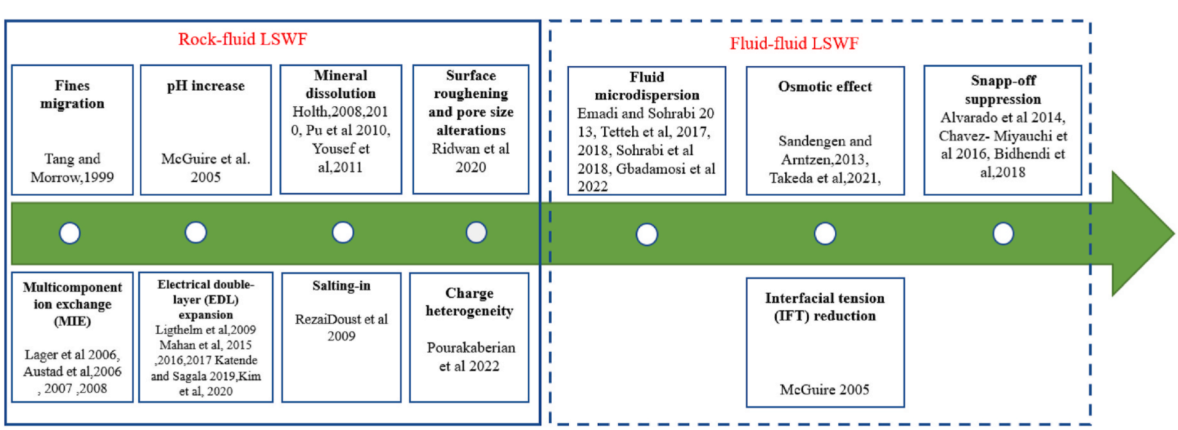

Fig. 2. Proposed timeline for LSWF mechanisms evolutions for wettability alteration during EOR.

throats and causes injected brine to diverge and flow in other paths, which in turn mobilize the residual oil from unswept areas, as shown in Fig. 3. However, this mechanism has contradicted various conducted experiments (Fathi et al., 2012; Lager et al., 2008a; Morrow and Buckley, 2011; RezaeiDoust et al., 2009; Zhang and Morrow, 2006; Zhang et al., 2007) that observed that no clay or very little clay was produced during their investigations and no clogging of pore throats with flow diversion. Thus, there is no relationship between clay migration and oil recovery improvement; clay may help wettability alteration (Liu and Wang, 2020).

2.1.2. pH increase

McGuire et al. (2005a) proposed this mechanism involving cation exchange between the clay and injected brine. Initially, organic and inorganic materials adsorb into the clay from the formation water, especially Ca^{2+}, to form a stable chemical equilibrium under reservoir pressure, pH, and temperature. After brine injection into the formation, equilibrium is disturbed between the brine and clay surface, and desorption of Ca^{2+} cations occurs. After that H^{+} proton adsorbs into the clay surface to fill the space left by Ca^{2+}, this leads to an increase in pH in the clay surface as described by Eq. (1), Ca^{2+} used as an example. This mechanism was also clarified by Austad et al. (2010a) with reference to Fig. 4.

$$Clay - Ca^{2+} + H_2O = Clay - H^{+} + Ca^{2+} + OH^{-} \tag{1}$$

After an increase in local pH near the clay surface, acidic-basic reactions occur between adsorbed basic materials and in-situ acidic materials, as shown in Eqs. (2) and (3). Due to these reactions, wettability changes to mixed wet or water wet; thus, crude oil is desorbed easily from the clay surface to increase the oil recovered (Austad et al., 2010a; Katende and Sagala, 2019).

$$Clay - NHR_3^{+} + OH^{-} = Clay + R_3N + H_2O \tag{2}$$

$$Clay - RCOOH^{-} + OH^{-} = Clay + RCOO^{-} + H_2O \tag{3}$$

For carbonate formation, acid and base reactions in the rock or pore surface cause carbonate minerals dissolution, leading to an increase in brine pH that, in turn, changes the oil-wet reservoir to mixed wet or water wet, leaving oil-free to flow towards the production well. Apart from that, this pH increase can initiate the natural surfactants (Bhicajee and Romero-Zerón, 2021; Yousef et al., 2011), which reduce interfacial tension, and emulsions formations for acidic oil to help recover residual oil saturation (Awolayo et al., 2018; Bhicajee and Romero-Zerón, 2021).

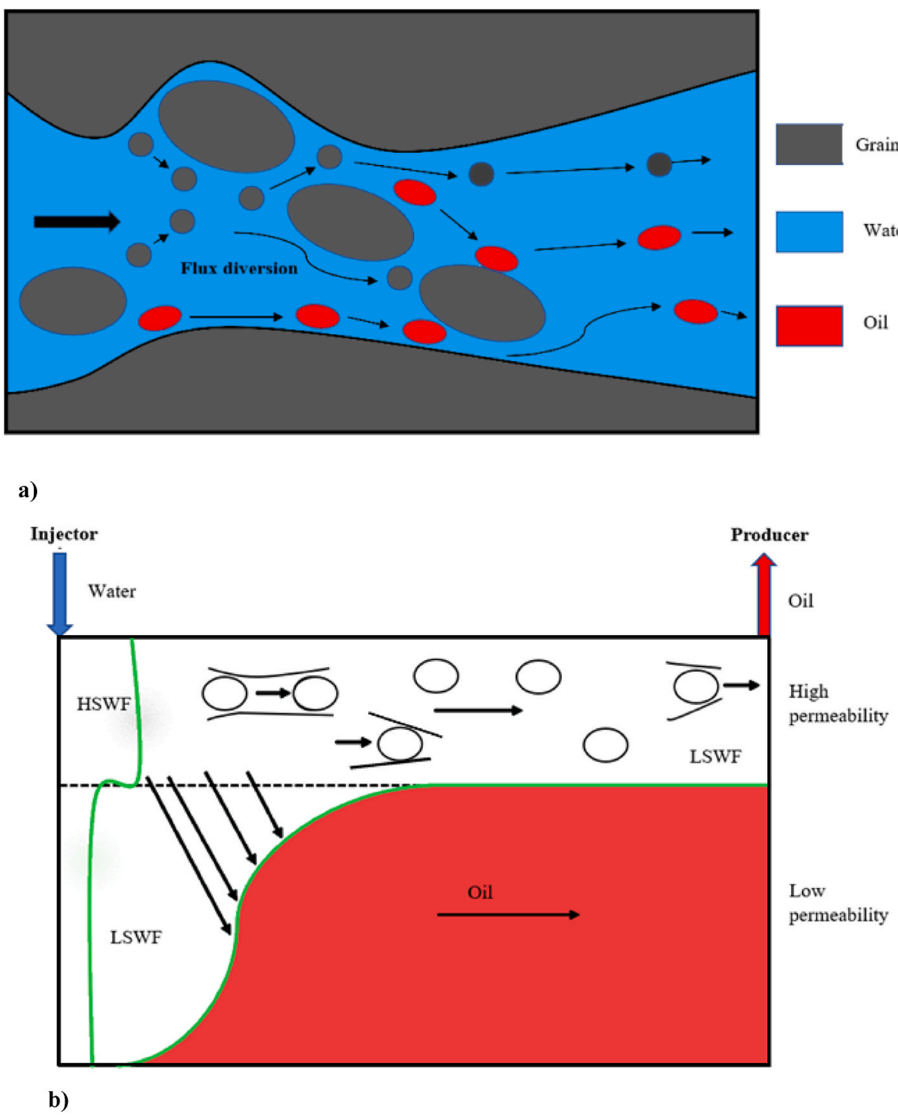

Fig. 3. (a)Fines migration and flux diversion due to formation damage (b)Oil recovery displacement in heterogeneous formation due to fines migration(Chequer et al., 2019; Dordzie and Dejam, 2021).

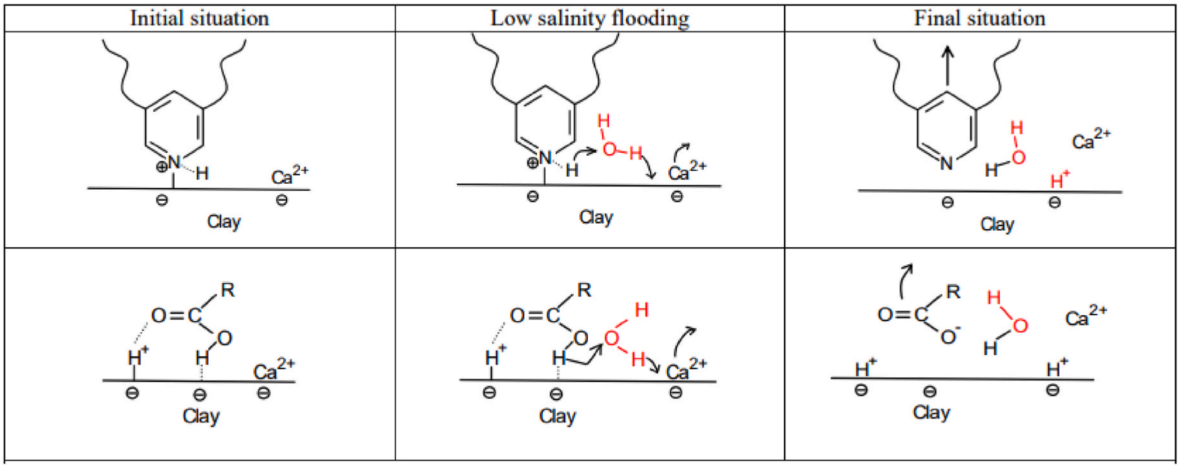

Fig. 4. pH increases effects on LSWF mechanism. Desorption of basic and acidic materials at the upper and lower parts (Austad et al., 2010a; Katende and Sagala, 2019).

2.1.3. Multicomponent ion exchange (MIE)

Lager et al. (2008b) proposed this LSWF mechanism, as shown in Fig. 5, whereby divalent cations, especially Ca^{2+} and Mg^{2+} from injected brine, trigger the desorption of organic compounds (positively and negatively charged) from the clay surface. The positively charged compounds from crude oil like N^{+} are adsorbed directly into clay negative surface through cation exchange. In contrast, divalent cations such as Ca^{2+} and Mg^{2+} bridge crude oil negatively charged acid components (carboxylate group) and clay surface negatively charged minerals through cation, ligand, and water bridging. The organic compound's adsorption mechanisms for MIE effects are shown in Table 2. This exchange enables increasing oil recovery due to the growing water-wet state. For MIE mechanisms to occur during LSWF, there must be polar components in the crude oil, clay minerals in the rock surfaces, and divalent cations in connate water. Seccombe et al. (2010) proved the MIE effects during LSWF, in which the oil rate increased as salt was reduced in injected water.

The possible equations for Multicomponent ion exchange (MIE) during LSWF are shown in Eqs. (4) and (5) for sandstones (Ridwan et al., 2020) and Eq. (6) for carbonates (Yutkin et al., 2022).

$$> Si - O - Mg - COO - R < +2Na^{+} \rightleftharpoons > Si - ONa + Mg^{2+} + NaCOOR < \quad (4)$$

$$> Al - O - Mg - COO - R < +2Na^{+} \rightleftharpoons > Al - ONa + Mg^{2+} + NaCOOR < \quad (5)$$

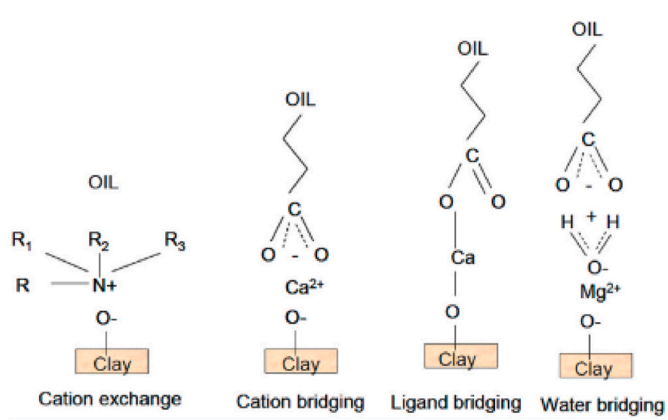

Fig. 5. Various adhesion mechanisms between polar components (crude oil) and clay surface (Lager et al., 2006).

Rock-Ion -Adsorbed oil + Ions ⇋ Rock -Ion + Releases Ion + Ion-Desorbed oil

$$2 > S^{-}Na^{+} + Ca^{2+} \overset{K_{CaNa}}{\rightleftarrows} > S_2^{2-}Ca^{2+} + 2Na^{+} \quad (6)$$

Where $2 > S^{-}$ represents the surface exchange site K_{CaNa} is the exchange equilibrium constant.

2.1.4. Salting-in effects

Salting-in is the process that involves decreasing the salt in the system. RezaeiDoust et al. (2009) proposed this LSWF mechanism which states that injecting low salinity brine in the reservoir disturbs the equilibrium between oil/water/rocks, which makes the polar organic material solubility in the water increase. Apart from that, some inorganic materials in injected water aid in breaking water molecules, thus increasing the solubility of organic materials. And this increases water wetness. This was verified through his experiments in which the solubility of 4-tert-butyl benzoic acid in an aqueous suspension of kaolinite increases with the decreasing salinity of brine used.

2.1.5. Mineral dissolution

Pu et al. (2010) proposed this mechanism after an experiment in sandstone with anhydrite cement over clay in Wyoming formations. Due to insignificant clay content, other mechanisms could not take place. Thus, after core flooding with brine having NaCl, the effluent contains SO_4^{2-},Na^{+}, Mg^{2+}, and K^{+}. The higher increase of SO_4^{2-} effluent was evidence for mineral dissolution process from anhydrite cement and has impacts on wettability change as well as permeability decrease after the release of dolomite crystals. Oil recovery increased from 5% to 8% OOIP for all tested cores.

Also, Pu et al. (2010) proposed this mechanism after an experiment for phosphoria dolomitic reservoir cores. After core flooding with brine

Table 2
Organic compounds adsorption mechanisms for MIE effects into minerals (Katende and Sagala, 2019).

No.	Mechanisms	Involved Organic functional groups
1	Cation exchange	Amino, ring NH, heterocyclic N (aromatic ring)
2	Protonation	Amino, heterocyclic N, carbonyl, carboxylate
3	Anion exchange	Carboxylate
4	Water bridging	Amino, carboxylate, carbonyl, alcoholic OH
5	Cation bridging	Carboxylate, amines, carbonyl, alcoholic OH
6	Ligand exchange	Carboxylate
7	Hydrogen bonding	Amino, carbonyl, carboxyl, phenolic OH
8	Van der Waals interactions	Uncharged organic units

having NaCl, the effluent contains SO_4^{2-} associated with decrease of permeability as supported by Lebedeva et al. (2009). High quantity of SO_4^{2-} effluent was the evidence for the mineral dissolution process from dolomite and has impacts on wettability change. The dissolution process resulted in a substantial increase in oil recovery through wettability alteration, as shown in Fig. 6.

2.1.6. Electrical double layer (EDL) expansion

Ligthelm et al. (2009) observed that, injecting low salinity brine with less multivalent cations when in contact with negatively clay surfaces, an electrical double layer (zeta potential) is developed and expands (diffuses) into oil. It develops a repulsive force that, when it exceeds the binding force of oil to the clay surface, wettability changes to mixed wet or water wet. For more clarification, refer to Fig. 7; when high salinity water, which contains more ions, is injected, the electrical double layer becomes more compact, whereas when low salinity water is injected, the electrical double layer expands, as shown in Fig. 7 (a) and 7 (b), respectively. The injected low-salinity water opens the layer, and Na^+ ions diffuse into an electrical double layer, as shown in Fig. 7 (c). The penetrated ions disturb the electrostatic forces between oil and clay and develop repulsive forces in between. And when these repulsive forces become higher than the binding forces between oil and clay, the bond between oil and clay is broken, wettability change to water wet, and oil is desorbed (Fig. 7 (d)) from the clay surface to increase oil recovery (Katende and Sagala, 2019).

From the laboratory and pilot/field tests, it has been revealed that oil recovery can be increased by changing the composition of injected brine during the injection process. This process is known as controlled salinity water flooding (CSW). Zeta potential is important in determining the optimal brine composition from oil-water interfaces and mineral-water interfaces. Zeta potential is the potential on the slipping plane at the point of the diffuse layer (Fig. 7). For the negatively charged oil-water interface, the injected brine must be modified to produce negative zeta potential on the mineral surfaces, which increases oil recovery. This can be accomplished by adding SO_4^{2-} ion concentration to the injected brine. In contrast, for the positively charged oil-water interface, the injected brine must be modified to produce positive zeta potential on the mineral surfaces to increase oil recovery. This is attained by adding Ca^{2+} or Mg^{2+} ions concentration in the injected brine(Jackson et al., 2016; Rahevar et al., 2023; Sagala et al., 2020; Shehata and Nasr-El-Din, 2015; Taleb et al., 2021).

2.1.7. Surface roughening and pore size alterations

Ridwan et al. (2020) investigated the effects of surface roughening and pore size of clay minerals during LSWF on increasing oil recovery in sandstone reservoirs. Modified -Ammott imbibition cell and low field

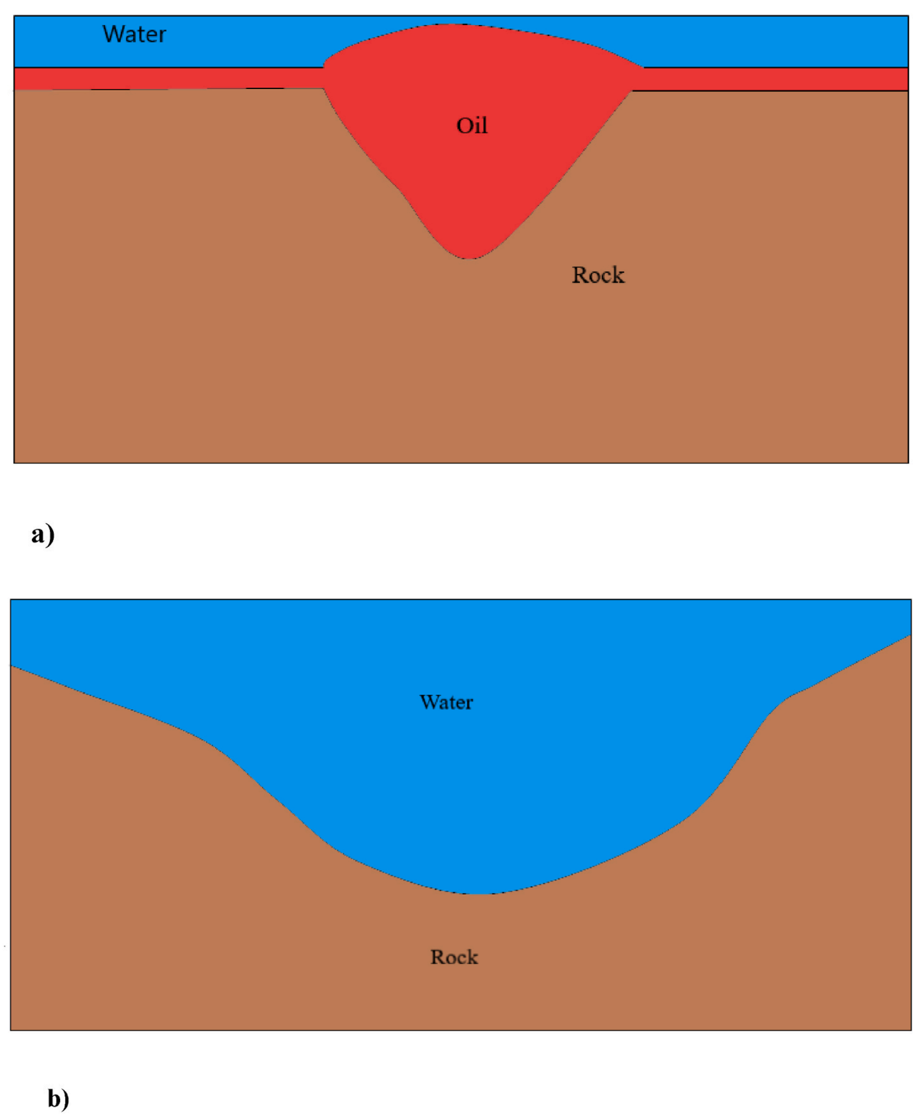

Fig. 6. Wettability changes due to mineral dissolution a) Before dissolution (oil-wet) b)After dissolution (water-wet) (Al-Shalabi and Sepehrnoori, 2016).

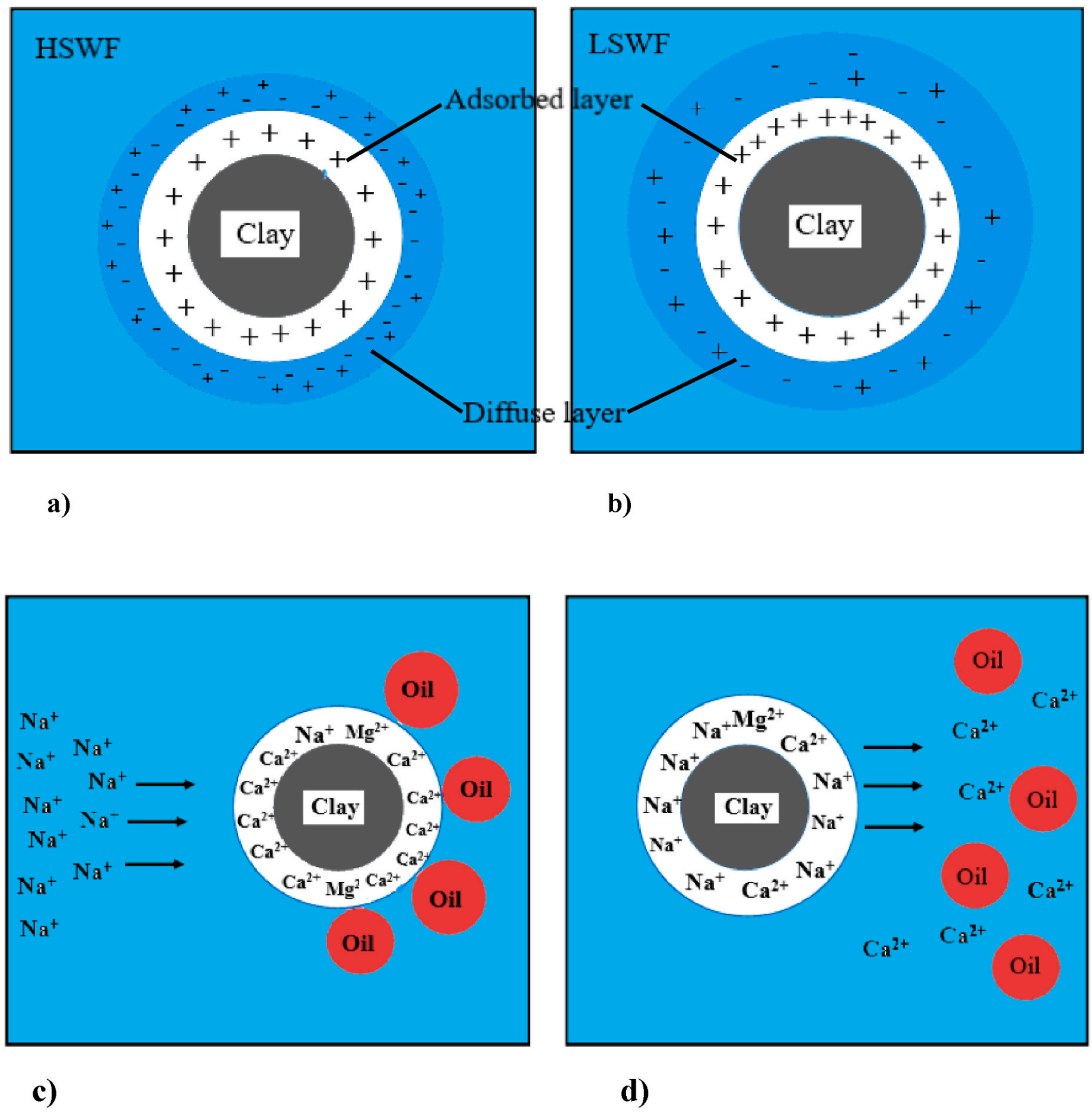

Fig. 7. Electrical double-layer expansion mechanism (Katende and Sagala, 2019).

nuclear magnetic resonance (NMR) were used to measure the oil recovered due to LSWF and deduction of pore size distribution during LSWF imbibition, respectively. It was revealed that when monovalent brine was injected into the core sample, it reduced pore size due to clay swelling and, thus, lower oil recovery. In contrast, divalent brine injection hinders the clay swelling, implying small pore size alteration and, therefore, higher oil recovery. In addition, monovalent ions result in higher recovery than divalent ions due to the higher surface roughness resulting from increased diffusion caused by increased tortuosity on the sandstone surfaces. The high electronegativity ions ($Mg^{2+} > Ca^{2+}$) from divalent ions tend to be attracted to the rock surface, which impedes surface roughness and thus lowers oil recovery.

2.1.8. Charge heterogeneity

Also, Pourakaberian et al. (2022) simulated film scale computational fluid dynamics (CFD) to postulate nanoscale physicochemical heterogeneities (surface roughness and charge heterogeneity) at the -oil--brine-rock (OBR) interface. Poisson-Nernst-Planck (PNP) equations were used and solved numerically between thin negative OBR interface systems (brine film). At high salinity water (HSW), the OBR interface was at equilibrium due to slow kinetics at the brine-thin film. In contrast, when low salinity water (LSW) was injected into the OBR system, EDL pressure became higher near the inlet film. It increased every area of the heterogeneous system rather than the homogeneous one, which creates disjoining pressure on the OBR system and depends on the heterogeneity of surface charges. Furthermore, LSW reduced the surface charge density at the OBR interfaces, thus weakening repulsive electrostatic force, which results in wettability change and an increase in oil recovery. However, surface roughness is more effective during HSWF, while charge heterogeneity is more pronounced during LSWF. This shows that heterogeneous surface charges can enhance LSWF; however, their extent depends on the surface roughness variation.

2.2. Fluid-fluid LSWF

2.2.1. Fluid microdispersion

Emadi and Sohrabi (2013) investigated the fluid-fluid interaction effects during LSWF after micromodel tests. It was revealed that when low salinity water is injected into reservoirs, larger water microdispersion (WMD) (dark particles) and partitioned (PRT) surface active materials are formed after contact with crude oil either at the interface or in crude oil. Because these dark particles are denser than crude oil, they move down to the clay surface and change the wettability to more water-wet by removing surface active materials, which causes an increase in oil recovery. These WMD and PRT were not formed with high water salinity flooding (HSWF); instead, oil surface active agents moved down and coalesced with the rock surface(Fig. 8 (a)), whereas, in LSWF, the active oil agents reacted with low salinity water to form micro-dispersion shown in Fig. 8 (b) causing oil to detach from the rock surface thus increase in water wet(Dordzie and Dejam, 2021). Furthermore, Darvish Sarvestani et al. (2019) found that microdispersion formation is independent of contact time. It depends on the extent of dilution of injected brine. For instance, ten times diluted seawater formed larger and greater number of emulsion droplets at zero and 10 h of contact with crude oil compared to seawater. Similar results have been reported by Maaref et al. (2017) in the micromodel scale.

2.2.2. Osmotic effect

Sandengen and Arntzen (2013) proposed this LSWF mechanism stating that when low salinity water is injected into the reservoir, oil act as a semi-permeable membrane allowing only pure water to diffuse into connate water, which expands after interactions, thus increase of oil recovery through this expansion process. This movement is because of the salinity difference (osmotic pressure) between injected water and connate water through a process known as osmosis, as shown in Fig. 9 (a to b, c to d). Later on, Fakcharoenphol et al. (2014b) supported this

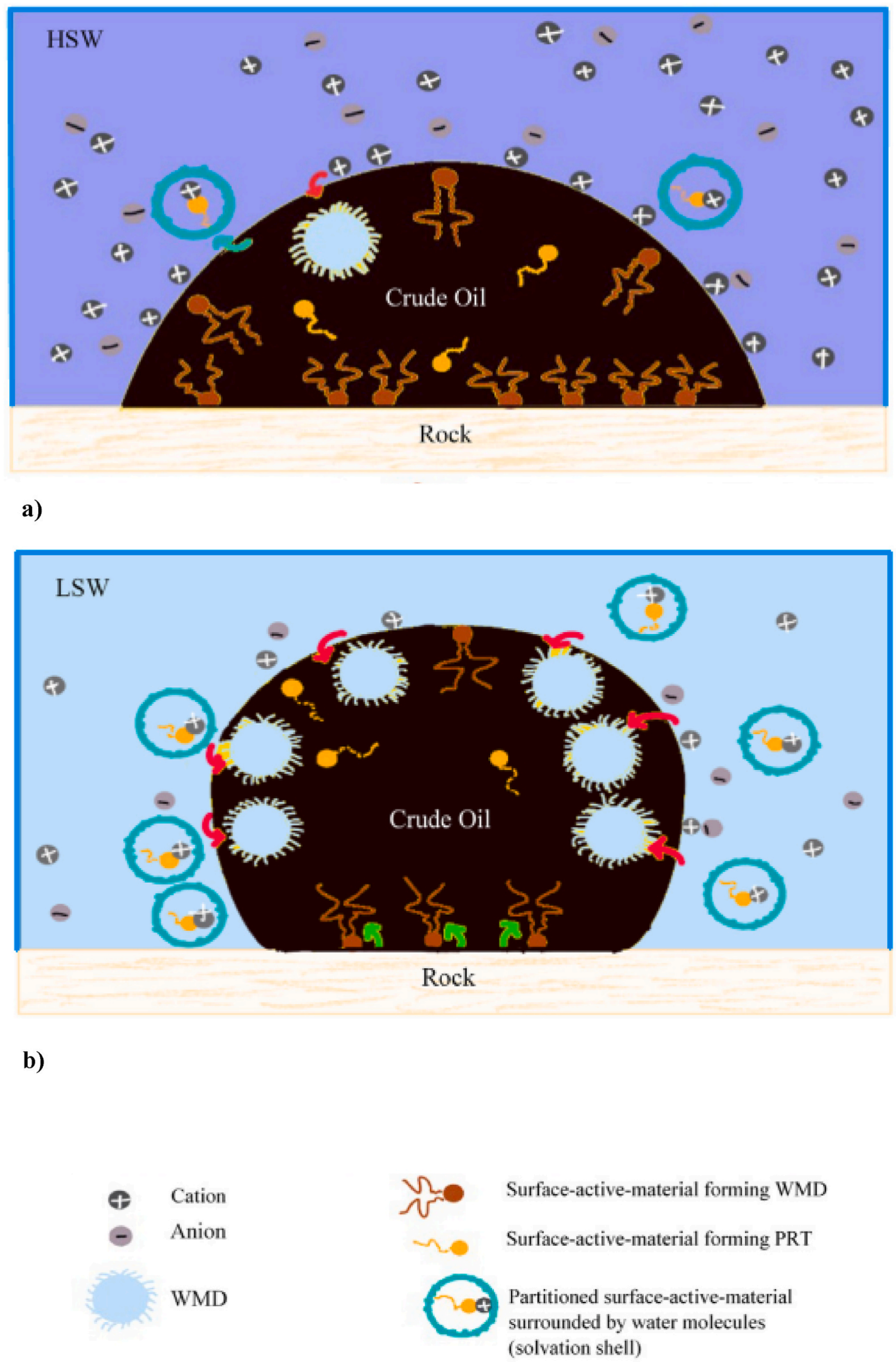

Fig. 8. Microdispersion formation a) HSWF b) LSWF(Dordzie and Dejam, 2021).

mechanism after laboratory experiments. In contrast, it was revealed that rock matrix especially acts as a semipermeable membrane. However, it depends on the rock type. Clay acts as a semipermeable membrane in shale formation (Fakcharoenphol et al., 2014a; Fredriksen et al., 2017b; Sandengen et al., 2016; Takeda et al., 2021).

2.2.3. Snap-off suppression

This LSWF mechanism demonstrated the effects of interfacial film effects formed between injected low water salinity and crude oil. The microfluid experiment conducted by Bidhendi et al. (2018) revealed that the interfacial film behaved like elasticity and exhibited breakage like a snap-off as the salinity of injected water reduced. Hence, the oil flow continues, and oil recovery rises. As shown in Fig. 10, oil effluent after snap-off for 0.01 salinity is larger than 0.1 and 1 fraction salinity.

2.2.4. Interfacial tension (IFT) reduction

This LSWF was proposed by McGuire et al. (2005b). After low salinity injected interacts with crude oil, the surfactants were formed from polar components. The process becomes like alkaline flooding, which reduces interfacial tensions, causing wettability change during the detachment of clay particles, thus reducing residual oil saturation. This mechanism is similar to surfactant flooding because IFT between water and oil is reduced, and pH elevation increases water wettability, increasing oil recovery. The difference between this and the surfactant mechanism is that surfactants are generated within the reservoir (in situ), i.e., not injected, but the action process remains the same. The surfactants generated disperse the oil into the water (emulsifying agent). In this context, the LSWF is similar to surfactant flooding and increases oil recovery. LSWF reduce the capillary number to a certain magnitude after changing wettability and reduction of IFT and it has proved that it has effects on recovering residual oil.

3. Experimental studies

Different researchers conducted several experiments to investigate various uncertainties on LSWF. These experiments helped to understand

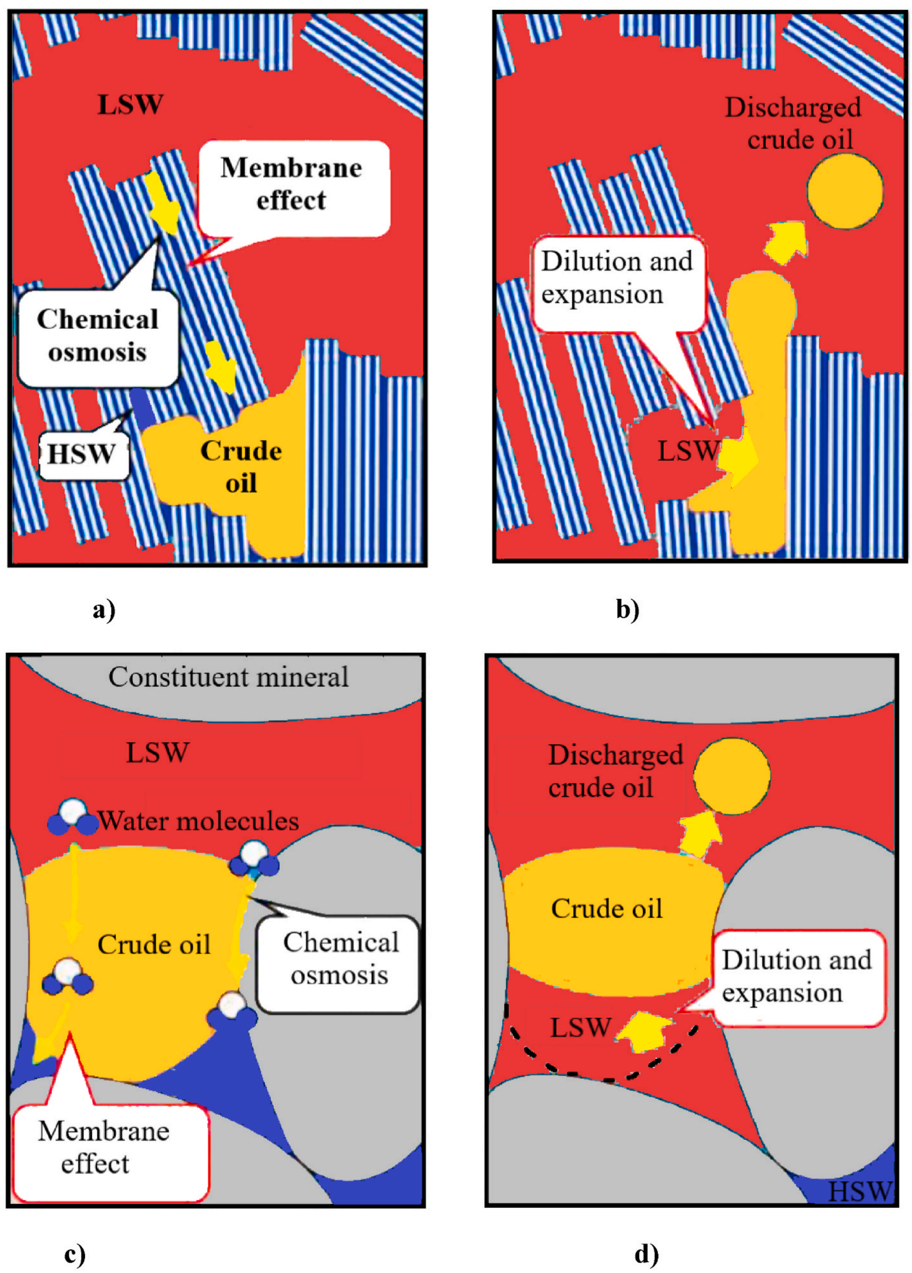

Fig. 9. Osmosis process during LSWF (Takeda et al., 2021).

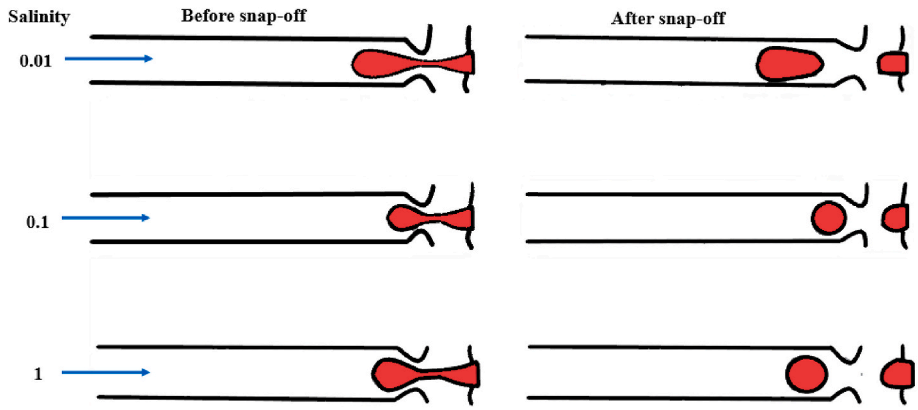

Fig. 10. Snap-off process for different salinity percentages (Bidhendi et al., 2018).

other underlying driving mechanisms for increasing oil recovery by injecting low-salinity water. They have recognized that wettability alteration triggered by rock-fluid, fluid-fluid, or rock-fluid-fluid interaction affects the LSWF process. Furthermore, the experiments generated different data for modeling and simulating the low-salinity flooding process. However, the mechanisms behind the wettability alteration are still unclear and contradict each other.

Mokhtari and Ayatollahi (2019) experimented IFT effects on wettability alteration effects on an increase in oil recovery. They used formation water and crude oil samples collected from the southwest of the Iranian oil reservoir field. Conductivity and pH tests of crude oil were performed on the aged water samples, while viscosity and density tests were performed on the aged crude oil samples. In addition, three distinct categories of IFT tests were created to clarify the LSWF primary mechanisms by considering (1) fresh brine-aged crude oil, (2) aged brine-fresh crude oil, and (3) aged brine-aged crude oil. Both pH and conductivity of all brine samples were tested at 25 °C using a Sper Scientific Bench-Top Meter Model 860032. In addition, after 45 days, UV–Vis and 1 H NMR spectroscopy were performed on aged brines. It was revealed that as the salinity of injected brine reduced, the dissociation with crude oil polar components increased. The results show relatively significant changes in oil viscosity, density, and IFT between crude oil and the 10 times diluted seawater in 45 days. These changes may substantially impact displacement efficiency after a significant time in the reservoir during LSWF. Besides that, UV–Vis and 1 H NMR spectroscopy show a higher concentration of naphthenic acids (NAs) for the 10 times diluted seawater compared to others, indicating the presence of higher amounts of NAs in the 10 times diluted seawater influence wettability changes compared to others.

Also, Mokhtari et al. (2019) experimented the role of fluid-fluid interactions in increasing oil recovery during LSWF using crude oil samples from Iranian reservoirs. In their experiment, formation water and crude oil were collected from the oil field, whereas brines water were prepared in the laboratory having different concentration by adding salts to deionized water as summarized in Table 3, followed by filtration through a 0.43 μm filter, then vacuumed to remove dissolved air. A synthesized glass was used during core flooding to avoid rock-fluid interaction wettability change. The results revealed that the dissolution of polar components from crude oil to brine is one of the driving mechanisms for increasing the oil recovery factor during LSWF. As the salt water dilution increases, oil recovery rises too. Also, 10SW brines recovered more oil than other brines because it significantly changes IFT and pH. IFT value for 10SW was minimum one (10.33 mN/m) compared to other brines, whereas its pH reduced from 7.45 to 4.22 after contacting with aging crude oil; and FW achieved the lowest pH value compared to other brines.2SW recover oil 83.25% of OOIP during secondary injection compared to 67.25% in tertiary injection. Similarly, 10SW brines recover more oil in the secondary phase than in tertiary phase injection. This concludes that the fluid-fluid interaction mechanism is more dominant in the secondary phase injection than in the tertiary phase.

Table 3
Laboratory prepared brines water (Mokhtari et al., 2019).

Salts	FW(ppm)	SW(ppm)	2SW(ppm)	10SW(ppm)
NaCl	140314	28424	14200	2842
KCl	0	825	400	82
$MgCl_2$	2854	6430	3215	642
$CaCl_2$	40286	1384	690	138
Na_2SO_4	2586	4490	2244	448
$NaHCO_3$	2014	106	84	10
$CaCO_3$	1628	0	0	0
TDS(ppm)	189682	41659	20833	4162
IS(mol/L)	3.674	0.832	0.416	0.0832

FW: Formation water; SW: Salinity water; TDS: Total dissolved solids.

Kim et al. (2020) experimented the effects of clay particles (kaolinite and illite) during low salinity water flooding in the Minnelusa formation in Powder River Basin. Three mechanisms investigated were pH increase, EDL expansion, and MIE. Before core flooding, low and high salinity were prepared based on NaCl concentration. Low salinity brines with 3000 ppm and high salinity brine with 30,000 ppm were used in the experiments with reference to formation water salinity having salinity ranges from 1134 to 261,982 ppm of NaCl.Also, TDS used in the experiment was 30,000 ppm. The experiment was conducted at room temperature (25 °C) to avoid fines migration. It was revealed that an oil recovery increase was more effective in kaolinite over illite clay particles. The oil recovery increase in kaolinite was 18%, whereas in illite was 6%. Furthermore, EDL and MIE showed positive responses to all clay particles. Apart from that, it was observed that pH increase increased oil recovery in both core samples. In addition, wettability change was observed more in kaolinite than illite core samples which changed to water wet. Also, correlation results revealed that kaolinite core samples had a strong relationship with all three LSWF mechanisms and oil recovery. In contrast, illite core samples showed a low correlation with EDL and MIE, except for an increased pH.

Mehraban et al. (2022) did a micromodel experiment to investigate fluid microdispersion effects and clay minerals on increasing oil recovery during LSWF. Two crude oil samples were chosen for core flooding, one with the ability to form microdispersion rich with acidic compounds such as asphaltenes, carboxylic acids, or related carboxylic functional groups and other crude oil with non-microdispersion compounds, both rich in clay minerals. It was revealed that when low salinity brine was injected in core samples, it interacted with surface charges of crude oil such as carboxylic acids or asphaltenes, which caused wettability changes and swelling of crude oil. For instance, in one of the experiments, 67.72% of OOIP was recovered during secondary high-salinity waterflooding. After tertiary LSWF oil increased to 73.10% of OOIP, i.e., 5.38% oil recovery increased due to microdispersion fluids effects. Furthermore, it was revealed that MIE and EDL are not primary mechanisms for LSWF, and clay particles did not significantly contribute to increased oil recovery. Also, critical observation from IR spectroscopy revealed that interactions between polar components from crude oil surface and low salinity brine significantly contribute to oil recovery increase, thus concluding that clay minerals which are rock-fluid interactions, are not enough to produce more oil during LSWF.

Al-Attar et al. (2013) experimented with analyzing the effects of low salinity brine and ionic composition to observe possible interactions of oil/brine/rock and other recovery mechanisms on carbonate core samples collected from the Bu Hasa Carbonate reservoir oil field in Abu Dhabi by using seawater. The additional two water was injected before, Um-Eradhuma with a salt concentration of 197,357 ppm and Simsima having 243,155 ppm, to analyze the mechanisms behind the increase in oil recovery. Before core flooding, Um-Eradhuma water was diluted to 5000 ppm, whereas Simsima was diluted to 1000 ppm by changing sulfate and calcium ions concentration. Wettability alteration was determined to be the driving mechanism for increasing oil recovery, confirmed through contact angle measurements. The wettability changes from oil-wet to intermediate water wet was observed with low salinity water injection. Also, it was revealed that reducing the salt concentration of injected brines from 197,357–5000 ppm resulted in an increase in oil recovery from 63% to 84.5% of OOIP. Different salt concentration with oil recovery is shown in Fig. 11. Only the sulfate ions concentration increase in brines changed wettability to intermediate water wet and oil recovery with optimal being 46.8 ppm in 5000 ppm brines. In contrast, calcium increase resulted in a decrease in oil recovery and more oil-wet. Besides, IFT was measured using an interfacial tensiometer with different salt concentrations during low brine core flooding. The results show that IFT has no systematic trends with salt concentration and oil recovery increase. This IFT result contradicts with that reported by Okasha and Al-Shiwaish (2009).

Austad et al. (2015) experimented the role of low salinity in enhancing oil recovery in limestone rocks containing anhydrite from the Middle East. Different effects, such as salinity, injection rate, and temperature, were analyzed on the anhydrite dissolution during LSWF. It was found that SO_4^{2-} concentration at the effluent increased as temperature decreased by 1.5, 2.8, and 3.4 mM at 130, 100, and 70 °C, respectively, with 130 °C appearing to be the equilibrium temperature. Also, the injection rate does not influence SO_4^{2-} concentration at the effluent. Furthermore, the dissolution of minerals in cores containing anhydrite is the primary driving mechanism in increasing oil recovery. It was added that more anhydrite ($CaSO_4^{2-}$) should be added, and sodium chloride (NaCl) decreased in injected brine for the wettability alteration process in carbonate formation. Because anhydrite was released as effluent, this confirmed the dissolution of anhydrite in the dolomite surface, which enabled a wettability change. Further, it was revealed that oil recovery increased by 33% of OOIP after 10 times diluted water injected compared to 25% and 30% of OOIP for water and seawater, respectively. This concludes that the dilution of brines enhances oil production in carbonate formation.

Mahmoudzadeh et al. (2022) did a microfluidics experiment to examine the LSWF mechanisms in fractured porous media in Iranian oil reservoirs. They used three different brines in their experiments: Formation water (FW), Seawater (SW), and low salinity water(LS). In the designed experiment, FW and SW, with TDS of 203000 ppm and 50000 ppm, respectively, were regarded as saline water, whereas 100SW water with TDS of 500 ppm was defined as low-salinity water. It was revealed that microdispersion formation is the dominant mechanism of wettability alteration in fractured porous media. Also, the results show that microdispersion formation is more effective in fractured porous media than porous media due to the diversion of low salinity from fractures to matrix formation when LS brines are injected over other water brines in oil and water wet formation. Furthermore, it was revealed that residual oil saturation after LSWF is small compared to different brine samples, as shown in Fig. 12.

Also, Mehdizad et al. (2022b) conducted micromodel tests investigating the role of clay swelling and migration-induced flow diversion combined with wettability alteration and osmotic effects on increasing oil recovery during LSWF for oil wet and water wet setup. In each micromodel test setup, each apparatus was coated with clays and others without clay to observe clay swelling and migration effects on increasing oil recovery. Heterogeneous porous sandstone media were created in a micromodel. To avoid clay flocculation during clay deposits in micromodel, NaCl with 15,0000 ppm solution was injected. Furthermore, NaCl and Sodium Bentonite mixture solution was injected in a micromodel to ensure better clay dispersion. NaCl in the mixture solution helps to provide better Sodium Bentonite adsorption in the micromodel surface. To make oil wet micromodel test, 2% of methyl trichlorosilane and 98% vol. toluene were injected for 10 min and then flooded with methane in an oven over 100 °C for 1 h later. The results revealed that clay migration flow diversion increased oil recovery by 30%, whereas 70% was due to wettability change and osmosis mechanisms in the oil

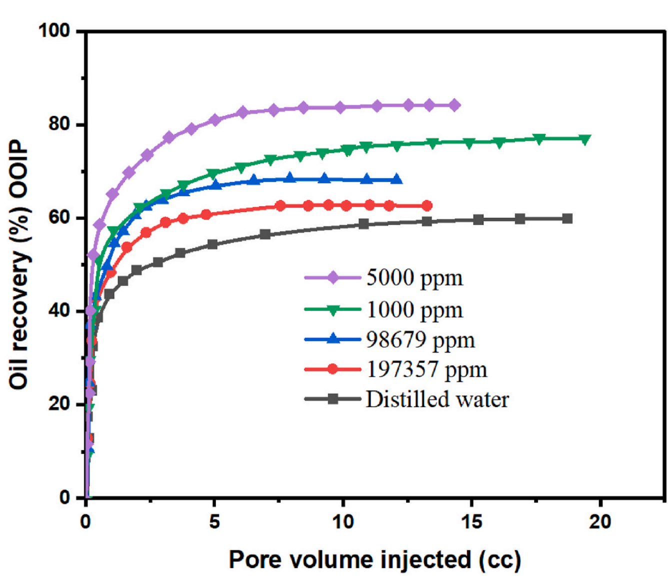

Fig. 11. Salt concentrations effects on RF (Al-Attar et al., 2013).

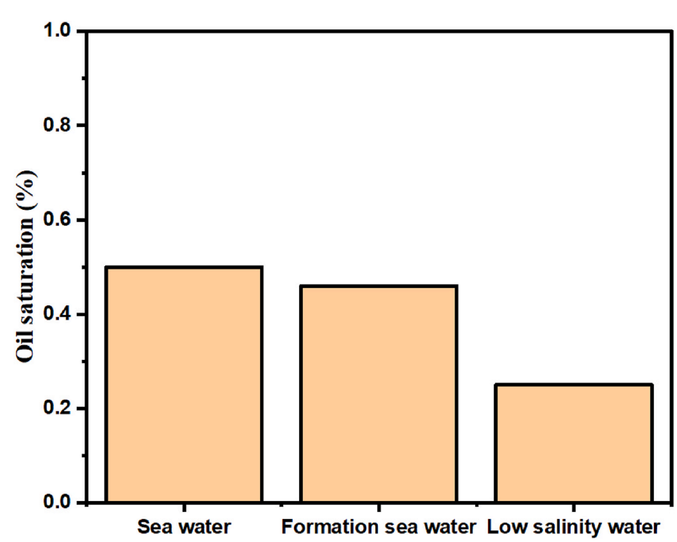

Fig. 12. Oil saturation versus different brines injected (Mahmoudzadeh et al., 2022).

wet system during LSWF. It was concluded that flow diversion contributes to oil recovery but is not a dominant mechanism.

Ebrahim et al. (2019) performed experiments to examine the effects of Silicon dioxide (SiO_2) nanoparticles in LSWF on increasing oil recovery. Different brines were prepared by adding different salt concentrations in distilled water, such as Potassium chloride (KCl), Sodium chloride (NaCl), Calcium chloride ($CaCl_2$), and Magnesium chloride ($MgCl_2$). SiO_2 was added to all mixed brines before flooding to a core enriched with crude oil. So in their study, one part of the experiment was conducted without SiO_2 and another with SiO_2. After core flooding, LSWF mechanisms were assessed by measuring zeta potential, contact angle, viscosity, and IFT. The results revealed that KCl and NaCl increased oil recovery more than $CaCl_2$ and $MgCl_2$. Also, SiO_2 addition in brines did not show any significant changes in IFT. Furthermore, SiO_2 decreased a contact angle from 11.7% to 8.26% by using different nanofluid concentrations from 0.1 to 0.02, which shows that SiO_2 influences wettability change from oil-wet to mixed water wet or to water wet that influences more oil recovery. Further, SiO_2 increased the viscosity of injected brines, which helped sweep more oil. In conclusion, by adding SiO_2 nanoparticles in injected brines recovered, 4% more oil was recovered than LSWF.

4. Modeling and simulations of LSWF

To successfully apply LSWF, modeling and simulation is essential stages to be conducted because they help to predict the amount of oil to be recovered after low salinity brine injection. Using collected data from experiments, several models have been built and simulated using various software to examine mechanisms that occur during LSWF. The steps to be followed for the modeling and simulation of LSWF are shown in Fig. 13. There are several established sets of equations to be considered when modeling and simulating LSWF in different simulating software like UTCHEM and SOLMINEQ.88, IPHREEQC, TOUGHREACT, Computer modeling group (CMG), Geochemist's Workbench, Schlumberger Eclipse, UTCHEM-IPHREEQC, KGEOFLOW, etc., taking into account different factors during LSWF(Dang et al., 2016b; Mwakipunda et al., 2023a; Opoku Boampong et al., 2023). Governing equations for LSWF are discussed in the next sub-sections.

4.1. Governing equations

Darcy's law and components diffusion govern flow, reaction kinetics, and equilibrium in porous media. The mass conservation equation for immiscible oil/water flow is given as follows (Qiao et al., 2016):

$$\frac{\partial}{\partial t}(\varphi S_\alpha \rho_\alpha) + \nabla.(\rho_\alpha \overrightarrow{u_\alpha}) = 0, \alpha = o, w \tag{7}$$

Where φ, S, ρ, and u represents porosity, saturation, density, and velocity, respectively.

Also, the flow rate is governed by Darcy's law given by Eq. (8):

$$\overrightarrow{u_\alpha} = \frac{k_{r\alpha}}{\mu_\alpha} K.\nabla(P_\alpha - \rho_\alpha g z), \alpha = o, w. \tag{8}$$

Here k represents permeability, μ is viscosity is gravitational constant, K is equilibrium constant, and P is pressure. Where subscripts *"w"* and *"o"* represent the oil and water phases. The capillary pressure and saturation between oil and gas are given in Eqs. (9) and (10), in which P_o and S_w are the primary unknown for the flow equations.

$$P_{cow} = P_o - P_w \tag{9}$$

$$S_o + S_w = 1 \tag{10}$$

For reactive transport, the mass conservation equation for the primary species p is given as:

$$\frac{\partial}{\partial t}\left(M_p + \sum_{q=1}^{N_{\sec}} v_{qp} M_q\right) + \nabla.\left(F_P + \sum_{q=1}^{N_{\sec}} v_{qp} F_q\right) = 0, p = 1, ..., N_p \tag{11}$$

The first and second terms represent the total moles accumulated and the total molar flux for primary components p. F stands for faradays constant, and M stands for molar density.

The conservation equation for the aqueous phase (oil and gas phase) of n_h components soluble in the aqueous phase is given as(Dang et al., 2016a, 2016b):

$$\psi_i \equiv \sum_{\alpha=o,g,w} \Delta T^u_\alpha y^u_{i\alpha}\left(\Delta p^{n+1} + \Delta P^u_{c\alpha} - \widetilde{\rho}^u_\alpha g \Delta d\right) + \sum_{q=o,g,w} \Delta D^u_{iq} y^u_{iq} + V\sigma^{n+1}_{i,aq} + q^{n+1}_i - \frac{V}{\Delta t}\left(N^{n+1}_i - N^n_i\right) = 0, i = 1, 2, ..., n_h; \tag{12}$$

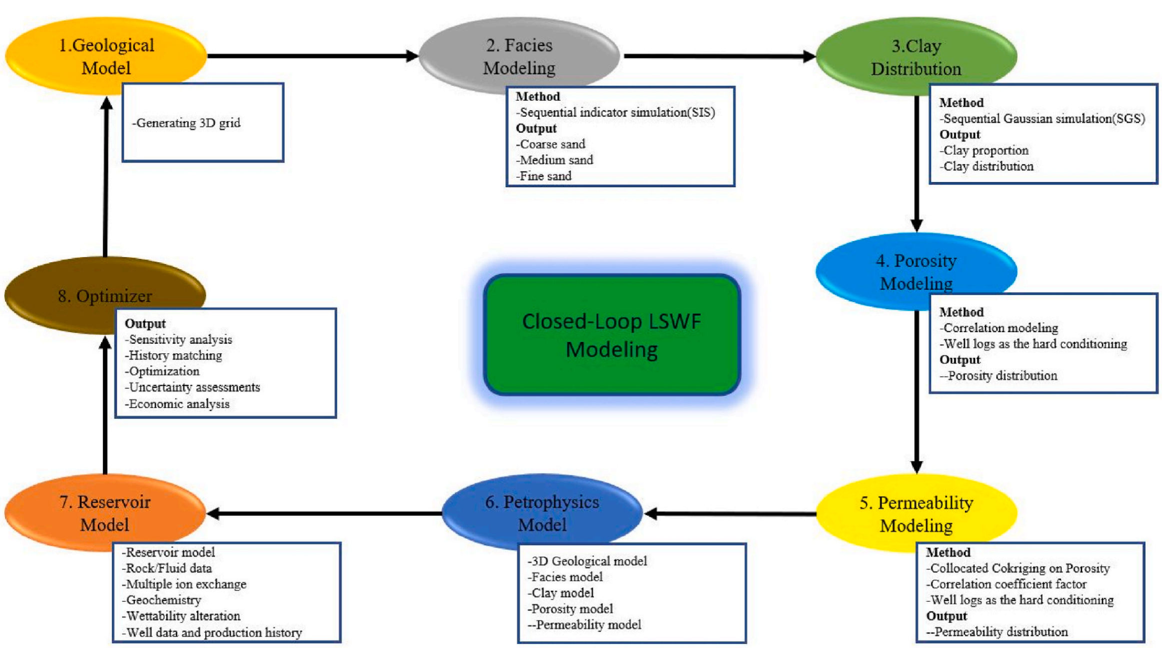

Fig. 13. Steps for modeling and simulating LSWF(Dang et al., 2016b).

For aqueous n_a components (ions), the conservation equation is given as follows:

$$\psi_j \equiv \Delta T_w^u y_{jw}^u \left(\Delta p^{n+1} - \widetilde{\rho}_w^u g \Delta d\right) + \Delta D_{iw}^u \Delta y_{iw}^u + V\sigma_{j,aq}^{n+1} + V\sigma_{j,mn}^{n+1} + q_j^{n+1} - \frac{V}{\Delta t}\left(N_{ja}^{n+1} - N_{ja}^n\right) = 0, j = 1, 2, ..., n_a; \tag{13}$$

For mineral components n_h, the conservation equation is given as follows:

$$\psi_k \equiv V\sigma_{k,mn}^{n+1} - \frac{V}{\Delta t}\left(N_k^{n+1} - N_k^n\right) = 0, k = 1, 2, ..., n_m; \tag{14}$$

Where n is the old time level, n+1 is the new time level. The u = n stands for explicit and n+1 for implicit blocks, as problems are solved based on the implicit solution. $V\sigma_{k,mn}^{n+1}$ stands for intra-aqueous reaction, $V\sigma_{i,aq}^{n+1}$ representing mineral reaction clarified in section number 4.2.

Thermodynamic equilibrium is given as the equality of fugacities in different phases (oil, gas, and aqueous) in Eqs. (15) and (16).

$$g_{i,1} \equiv f_{ig} - f_{io} = 0, i = 1, ..., n_h, \tag{15}$$

$$g_{i,2} \equiv f_{ig} - f_{iw} = 0, i = 1, ..., n_h, \tag{16}$$

Where f_{ig} and represent gas fugacity calculated by Peng-Robin equation and f_{iw} stands for gaseous components soluble in aqueous phase computed from Henry's law given in Eq. (17).

$$f_{iw} = y_{iw} H_i \tag{17}$$

Where H_i is Henry's constant for different components y_{iw}.

The constraint volume equation for compositional simulation is given in Eq. (18).

$$\sum_q \left(\frac{N_q^{n+1}}{\rho_q^{n+1}}\right) - \varphi^{n+1} = 0, q = o, g, w \tag{18}$$

4.2. Intra-aqueous and mineral reactions

The CO_2 sequestration geochemical reactions proposed by Nghiem et al. (2004) are used to model LSWF intra-aqueous and mineral reactions such as MIE. At equilibrium, forward and backward reactions are equally given in as (Dang et al., 2016a, 2016b; Nghiem et al., 2004):

$$Q_\alpha - K_{eq,\alpha} = 0, \alpha = 1, ..., R_{aq} \tag{19}$$

$$Q_\alpha = \prod_{k=1}^{n_{aq}} (a_k)^{v_{k\alpha}} \tag{20}$$

Where K_{eq} represent the chemical equilibrium constant given by Kharaka et al. (1988) and depends on temperature, Q_α activity product, number of species, and stoichiometric constant.

Solution concentration is directly related to the activities of each species. To reduce errors, activities of water and mineral are set to one.

$$\alpha_i = \gamma_i m_i, i = 1, ..., n_{aq} \tag{21}$$

Where α_i is the activity of species, m_i is concentration in solution, and γ_i is activity constant, which is assumed to be one for ideal cases.

The mineral dissolution or precipitate assumed to occur instantaneously is computed by Eq. (22) with the Equilibrium rate annihilation (ERA) matrix speeding the computing efficiency(Nghiem et al., 2004, 2011).

$$r_\beta = \widehat{A}_\beta k_\beta \left(1 - \frac{Q_\beta}{K_{eq,\beta}}\right), \beta = 1, ..., R_{mn} \tag{22}$$

Where $\widehat{A}_\beta$ is the reactive surface area of reactant(m^2/m^3), k_β is the mineral reaction rate constant(mol/m^2s), $K_{eq,\beta}$ is the chemical equilibrium constant for either mineral precipitation or dissolution reaction, Q_β is activity product of mineral, r_β is mineral dissolution/precipitation rate (mol/m^3s).

The mineral reaction rate depends on temperature and is calculated using Eq. (23).

$$k_\beta = k_{0,\beta} \exp\left[-\frac{E_a}{R}\left(\frac{1}{T} - \frac{1}{T_0}\right)\right] \tag{23}$$

Where E_a is activation energy (J/mol), R is the universal gas constant which is (8.314 J/mol K) $k_{0,\beta}$, and is the reaction rate constant at initial temperature T_0 (K).

Also, the reactive surface area of the reactant, which changes when it dissolves or precipitates, is given by Eq. (24).

$$\widehat{A} = \widehat{A}_0 \cdot \frac{N_\beta}{N_{\beta 0}} \tag{24}$$

Where $\widehat{A}_0$ is the reactive surface area at the initial time, $N_{\beta 0}$ and N_β are the number of moles in grid blocks at an initial and current time, respectively.

4.3. Ion's exchange

As brine is injected into the reservoir, the ion exchange occurs with connate water. Because chemical equilibrium is disturbed after LSWF, two reversible reactions involving ions exchange Na^+, Ca^{2+}, and Mg^{2+} occur, expressed in Eqs. (25) and (26) (Dang et al., 2016a, 2016b; Nghiem et al., 2011; Omekeh et al., 2012).

$$Na^+ + \frac{1}{2}(Ca - X_2) \rightleftharpoons (Na - X) + \frac{1}{2}Ca^{2+} \tag{25}$$

$$Na^+ + \frac{1}{2}(Mg - X_2) \rightleftharpoons (Na - X) + \frac{1}{2}Mg^{2+} \tag{26}$$

The ion exchange in the clay surface is modeled using selectivity coefficients given in Eqs. (27) and (28).

$$K'_{Na/Ca} = \frac{\zeta(Na - X)[m(Ca^{2+})]^{0.5}}{[\zeta(Ca - X_2)]^{0.5} m(Na^+)} \times \frac{[\gamma(Ca^{2+})]}{\gamma(Na^+)} \tag{27}$$

$$K'_{Na/Mg} = \frac{\zeta(Na - X)[m(Mg^{2+})]^{0.5}}{[\zeta(Mg - X_2)]^{0.5} m(Na^+)} \times \frac{[\gamma(Mg^{2+})]}{\gamma(Na^+)} \tag{28}$$

4.4. Wettability alteration modeling

Wettability change during LSWF is modeled by using relative permeability changes shift curves. Two curves, one for high salinity and the other for low salinity are used to interpolate the third curve, as shown in Fig. 14 (Dang et al., 2016b). Mathematically is given by Eq. (29) (Dang et al., 2013, 2016a; Shojaei et al., 2015). Also, Tripathi and Mohanty (2008) established their model to investigate wettability alteration during LSWF. Besides, θ could be estimated using the maximum energy barrier system if data are available, as shown in Eq. (30) (Jadhawar and Saeed, 2023).

$$\theta = \frac{S_{orw} - S_{orw}^{LS}}{S_{orw}^{HS} - S_{orw}^{LS}} \tag{29}$$

$$\theta = \frac{MEB - MEB_{\min}}{MEB_{\max} - MEB_{\min}} \tag{30}$$

Where θ is the interpolant value (scaling factor). MEB, $MEB_{min,}$ and MEB_{max} represent the existing maximum energy, the lower limit of existing maximum energy, and the upper limit of existing maximum energy obtained from relative permeability experimental curves. Then scaling factor is used to compute altered relative permeability and residual oil saturation as follows:

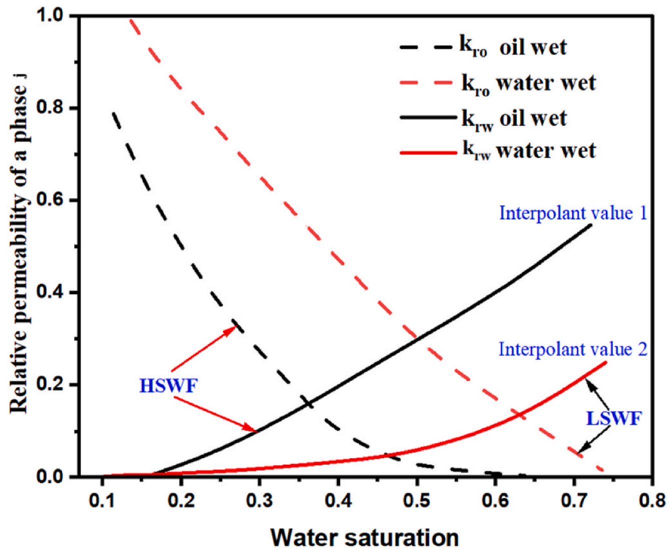

Fig. 14. Shift of curves used to model wettability change during LSWF(Dang et al., 2016b).

$$k'_{rw} = \theta \times k^{ww}_{rw} + (1-\theta) \times k^{ow}_{rw} \tag{31}$$

$$k'_{ro} = \theta \times k^{ww}_{ro} + (1-\theta) \times k^{ow}_{ro} \tag{32}$$

$$S'_{orw} = \theta \times S^{ww}_{rw} + (1-\theta) \times k^{ow}_{orw} \tag{33}$$

Where k'_{rw}, k'_{ro}, and S'_{orw} represent altered water relative permeability, oil relative permeability, and residual oil saturation, respectively. $k^{ww}_{rw}k^{ww}_{ro}$, and S^{ww}_{rw} stands for altered water relative permeability, oil relative permeability, and residual oil saturation, respectively. Also, *ow* and *ww* represent oil wet and water wet values. However, in most simulation studies, the capillary pressure change is neglected. Instead, relative permeability curves form a crude-oil-brine-rock (COBR) model for flow condition simulation.

Aljaberi et al. (2022a) established a semi-empirical model that can predict relative permeability data during LSWF based on oil recovery increase and pressure change. The model can be applied to all types of rocks, fluid conditions, and wettability changes regardless of the dominant driving mechanisms. Their model was used to validate experimental core flood data. The porosity and permeability of the model were assumed to be homogeneous. CMG-STAR was used to build one dimensional model and CMG-CMOST to generate initial relative data permeability through history matching. A black oil simulator matched the initial fluids used in the experiments to prevent mass transfer complexity in the model. The results revealed that the model built could be used to predict oil recovery increase and pressure changes in secondary and tertiary stages of oil production. Furthermore, it gives the LSWF relative permeability data in secondary and tertiary, regardless of active mechanisms.

Sharma and Mohanty (2018) did a simulation study based on experimental data to investigate rock-fluid interactions during LSWF in carbonate formation using UTCHEM-IPHREEQC software. It was based only on geochemical interactions. Three wettability alterations mechanisms were mineral dissolution (calcite and anhydrite), dolomitization on the rock surface, and sulfate adsorption. The model assumed that: 1) Calcite surfaces comprise calcium and carbonate-charged particle sites interacting with calcium, magnesium, and sulfate ions to complete required reactions.2) The complex surface reactions occur between the unveiled lattice bound ions with water and other dissolved materials.3) The extent of oil wetness depends on the organic materials attached to the rock surface, which is a function of geochemical reactions of the syststem.4)Local equilibrium was assumed in the model to allow interactions and reactions in aqueous phase between primary surfaces species and dissolved ions. The most important reactions included in the model are shown in Table 4. The results revealed that the simulation studies match the experimental data, as shown in Figs. 15 and 16 for oil recovery prediction and zeta potential measurements, respectively. Also, three wettability alterations mechanisms, mineral dissolution (calcite and anhydrite), dolomitization on the rock surface, and sulfate adsorption, were recognized in the model. This cement that UTCHEM-IPHREEQC can be used to model geochemical interactions.

Hien et al. (2021) conducted a simulation based on experimental data using MATLAB software in the Nam Con Son Basin, Vietnam. Multicomponent ion exchange (MIE) LSWF mechanism was considered in their finite volume element-based developed model. The results revealed that the oil recovery increased by 2.19% for the lower Miocene sand formation. Furthermore, the proposed simulation results matched the experimental data, as shown in Fig. 17. However, they did not consider capillary pressure effects in their developed model (codes), which was recommended for future studies.

Brantson et al. (2020b) developed a model by using MATLAB software which can be used for predicting oil recovery performance in heterogeneous porous media during LSWF. MIE was coupled in the model as the main driving mechanism for wettability alteration. A hybrid particle swarm optimization artificial neural network (PSO-ANN) was used for recovery factor prediction. PSO-ANN with 7 inputs, 3 hidden layers, and 1 output was validated with PHREEQC geochemical numerical simulator. The inputs for the model were simulation time, porosity, permeability, water saturation, polymer concentration, salt concentration, and reservoir pressure, whereas output was the recovery factor. There was a significant correlation between the PHREEQC simulator and a developed numerical simulator. Also, it was revealed that PSO-ANN could be used as an alternative for recovery factor prediction because it uses less computational time with less than 1% average absolute percentage error (AAPE) during the training and testing of the model. Shafiei et al. (2022) used machine learning techniques to predict recovery factors during LSWF in carbonate oil formations. The inputs for the model were brine permeability, porosity, HCO_3^- concentration, salinity of the connate brine, residual water saturation of the core,the salinity of the injected brine, core diameter. Initial recovery

Table 4
Reactions used to build the model in UTCHEM-IPHREEQ with k values (Sharma and Mohanty, 2018).

S/N	Aqueous reactions	Constants
1	$HA = H^+ + A^-$	Log k = 3.98
2	$Ca^{2+} + A^+ = CaA^+$	Log k = −2.2
3	$Mg^{2+} + A^- = MgA^+$	Log k = −3.3
4	$Ca^{2+} + SO_4^{2-} = CaSO_{4\,(aq)}$	Log k = 2.25
5	$Mg^{2+} + SO_4^{2-} = MgSO_{4\,(aq)}$	Log k = 2.37
6	$HCO_3^- = H^+ + CO_3^{2-}$	Log k = −10.39
7	$CO_3^{2-} + 2H^+ = CO_2 + H_2O$	Log k = 16.68
Dissolution/Precipitation reaction		
8	$CaCO_{3(s)} = Ca^{2+} + CO_3^{-2}$	Log k = −8.48
9	$CaMg(CO_3)_{2(s)} = Ca^{2+} + Mg^{2+} + 2CO_3^{2-}$	Log k = −17.09
10	$CaSO_{4(s)} = Ca^{2+} + SO_4^{2-}$	Log k = −4.58
Surface complexation reactions		
11	$> CaH_2O^+ + A^- => CaH_2OA$	Log k = 0.4
12	$> CaH_2O^+ => CaOH + H^+$	Log k = −12.8
13	$> CaH_2O^+ + HCO_3^- => CaCO_3^- + H^+ + H_2O$	Log k = −5.65
14	$> CaH_2O^+ + HCO_3^- => CaHCO_3^- + H_2O$	Log k = 1.68
15	$> CaH_2O^+ + SO_4^{2-} => CaSO_4^- + H_2O$	Log k = 3.3
16	$> CO_3^- + H^+ => CO_3H$	Log k = 5.48
17	$> CO_3^- + Ca^{2+} => CO_3Ca^+$	Log k = 1.74
18	$> CO_3^- + Mg^{2+} => CO_3Mg^+$	Log k = 1.74
19	$> CO_3Ca^+ + SO_4^{2-} => CO_3CaSO_4^-$	Log k = 3.3
20	$> CO_3Mg^+ + SO_4^{2-} => CO_3MgSO_4^-$	Log k = 3.3
21	$> CO_3Mg^+ + A^- => CO_3MgA$	Log k = 0.4
22	$> CO_3Ca + A^- => CO_3CaA$	Log k = 0.4

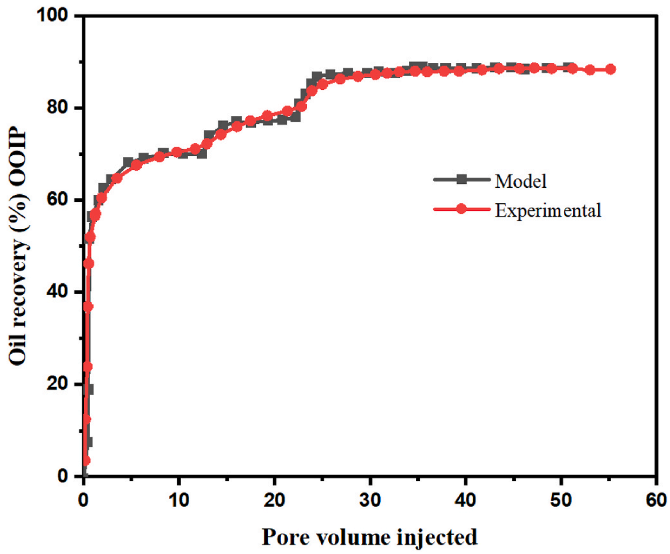

Fig. 15. Experimental versus simulation study (Sharma and Mohanty, 2018).

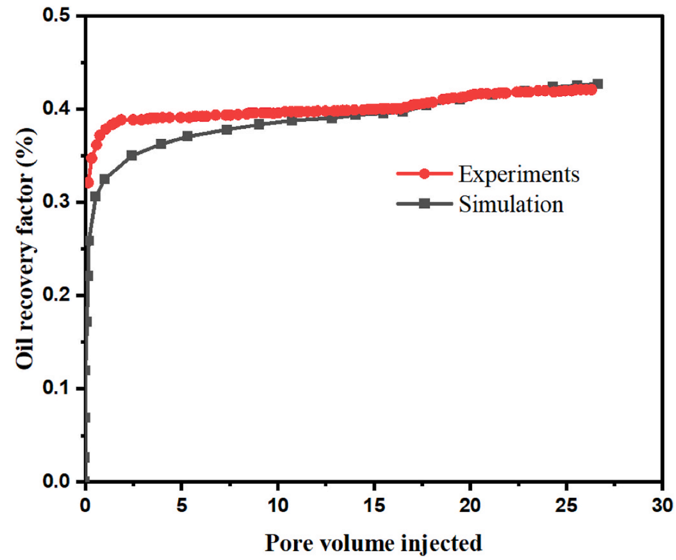

Fig. 17. Experimental versus simulation results (Hien et al., 2021).

factor was used as output of the model. The machine learning used to develop models were support vector machine (SVM), artificial neural networks (ANNs), decision trees (DT), Committee Machine Intelligent System (CMIS), and random forest (RF). The models' performances are shown in Table 5. From Table 5, it was revealed that RF outperformed other models in predicting oil recovery factors, hence should be adapted for predicting oil recovery performances in LSWF.

Olabode et al. (2020) used Schlumberger ECLIPSE software's black oil simulator to model and simulate LSWF immediately after secondary energy depletion. The model was assumed to be homogeneous with average porosity and permeability of 0.25 and 200 mD, respectively. Two horizontal producer wells located at coordinates (15,15) with one injector well located at coordinates (1,1) at a depth of 2600 m were used to produce and inject low salinity brine, respectively, both at a rate of 100 m^3/day. The simulations were run for 25 years with a high salinity of 30 ppm, followed by different low salinity concentrations. Oil recovery increased by 22.66%, production rate by 35.12%, and water cut reduced by 26.77% when low salinity brines injected into the reservoir. Dang et al. (2015) modeled and optimized low salinity waterflood using CMG-GEM™ and CMOST™ reservoir simulator in a sandstone reservoir. The developed model considered all geochemical reactions responsible for wettability change by shifting the relative permeability curve from oil-wet to water-wet conditions. Also, a developed model considers clay

Table 5
Models performances for oil recovery factor prediction (Shafiei et al., 2022).

Model	Subset	R^2	RMSE (%)	MARD (%)	SD (%)	MRD (%)	N
ANNs	Training	0.8214	5.959	3.629	5.959	0.277	388
	Testing	0.6984	8.436	4.314	8.434	−0.373	98
	Total	0.7893	6.534	3.767	6.534	0.146	486
CMIS	Training	0.8794	4.898	2.793	4.896	0.343	388
	Testing	0.8049	6.460	3.685	6.419	0.789	98
	Total	0.8628	5.251	2.973	5.245	0.433	486
RF	Training	**0.9722**	**2.497**	**1.461**	**2.496**	**0.201**	**388**
	Testing	**0.8399**	**5.757**	**3.302**	**5.753**	**0.559**	**98**
	Total	**0.9445**	**3.415**	**1.832**	**3.415**	**0.273**	**486**
DT	Training	0.9996	0.293	0.027	0.293	0.000	388
	Testing	0.7645	7.117	4.030	7.116	0.163	98
	Total	0.9491	3.207	0.834	3.207	0.033	486
SVM	Training	0.8772	5.064	2.883	5.056	0.203	388
	Testing	0.7937	6.534	3.768	6.521	0.754	98
	Total	0.8587	5.393	3.061	5.391	0.314	486

R^2: Correlation coefficient; RMSE: Root mean squared error; MARD: Mean absolute relative deviation; SD: Standard deviation; MRD: Mean relative deviation; N: Total data.

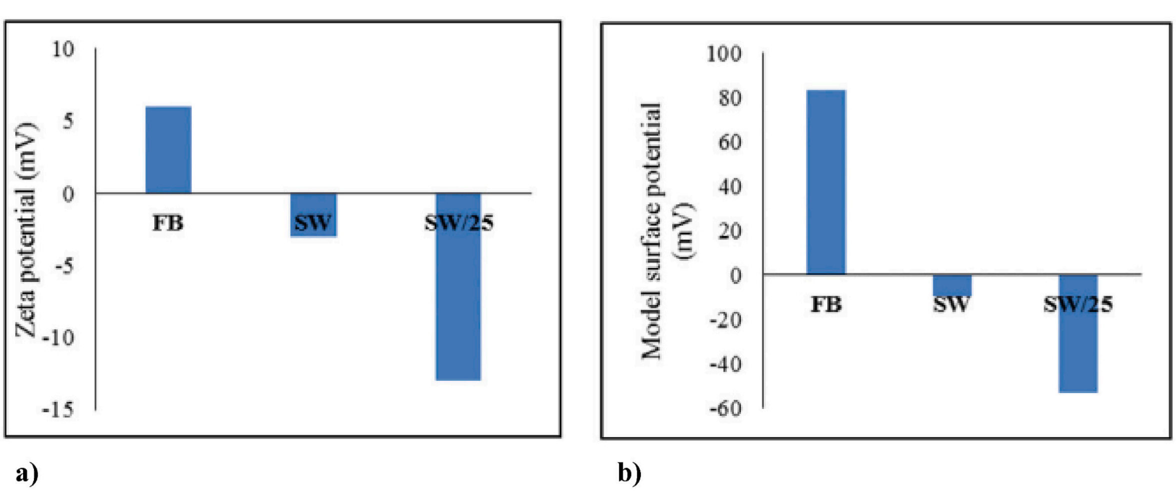

Fig. 16. Zeta potential from **a)** Experimental b) Modeling(Sharma and Mohanty, 2018).

content and distribution effects in oil recovery using the equation of state compositional reservoir simulator. Then, Infill drilling optimization by using low-salinity brine injection was implemented. The results revealed that the experimental core flood matched the proposed simulation results for oil recovery and pressure drop as shown in Fig. 18. Furthermore, it was concluded that fines migration is one of the important aspects in LSWF.

5. Hybrid low salinity waterflooding

Hybrid LSWF combines low-salinity brine with other EOR techniques to increase oil recovery. Many laboratory experiments have been conducted in sandstone and carbonate formations to investigate the driving mechanisms behind the process. This section analyzes the effects of combining LSWF with other techniques on recovering residual oil saturation.

Hossein Javadi and Fatemi (2022) did a core flooding experiment on hybrid LSWF by considering fluid-fluid interaction effects on increasing oil recovery in fractured porous reservoirs. They used low-salinity water and surfactant. Cationic surfactant cetyltrimethylammonium bromide (CTAB) (Fig. 19) was added in different low water salinity concentrations (Table 6), to observe their oil recovery effectiveness. In the experiment, core flooding of low salinity brines was initially conducted without CTAB, followed by core flooding having a CTAB. As shown in Fig. 20, it was revealed that before CTAB application in salinity water, 10dSW outperformed other diluted brine salinity. However, after CTAB application to the salinity water having 1000 ppm, SW + 1000 ppm CTAB surpassed other diluted brines with CTAB. This shows that before the CTAB application, the dominant mechanism was wettability alteration confirmed through zeta potential and IFT measurements. Then after CTAB addition, the driving mechanisms were due to surfactants' ability to detach polar components in the region between brines and oil to form emulsions based on the van der Waals hydrophobic forces.

Also, Sami et al. (2022) used natural surfactants extracted from Avena Sativa (oat) with low salinity water to investigate their effects on increasing oil recovery during LSWF. The physical and chemical characteristics of Avena showed that it is stable and efficient and thus can be used for enhanced oil recovery with nonionic saponin. Different salts were used during the experiments: NaCl, KCl, $MgSO_4$, Na_2CO_3, $MgCl_2$, $CaCl_2$, Na_2CO_3, Na_2SO_4, and $NaHCO_3$ to asses the functions of each ion during LSWF. Deionized water (DIW) and diluted seawater DSW2000 were used in their experiments with natural surfactants having a critical micelle concentration (CMC) of 4000 ppm. Na_2CO_3 was more compatible with natural surfactants from all the listed salts than others, with an IFT reduction to 1.38 mN/m, whereas MgSO4 had the least compatibility with natural surfactants, with an IFT reduction to 6.63 mN/m. In contact angle measurements, when the CMC of natural surfactants was used, it reached 38.28° with Na_2CO_3, 55.12° for DSW2000, and 82.60° for $MgSO_4$.In addition, it was found that a combination of Na_2CO_3 low brines with natural surfactants (nonionic) increased the oil recovery factor by 28.89% during LSWF in the tertiary stage, 23.14% by DSW2000, and 18.3% by NaCl.

Also, Al-Saedi et al. (2020) conducted experiments and simulations to investigate the effects of low salinity and steam flooding (LSASF) on increasing oil recovery for the Bartlesville Sandstone. Reservoir core samples were characterized by a high oil viscosity of 600 cP and average permeability of 80 mD. Different measurements were used to assess the new hybrid low salinity water, such as contact angle measurements, IFT measurements, imbibition tests, zeta potential measurements, and the reactive transport model. It was revealed that LSASF increased oil recovery more than LSWF, as shown in one of the designed experiments, Fig. 21. This is because steam sweeps residual oil saturation easily by lowering oil viscosity, increases permeability due to mineral dissolution, and changes in wettability which boost spontaneous imbibition., etc. Also, it was observed that as salinity decreases, zeta potential decreases, and contacts angle confirmed that oil wet changes to more water-wet

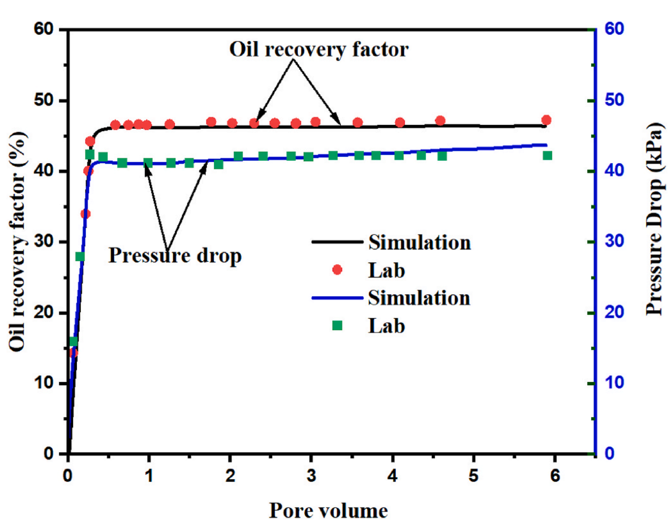

Fig. 18. Proposed model simulations vs. Laboratory experiments (Dang et al., 2015).

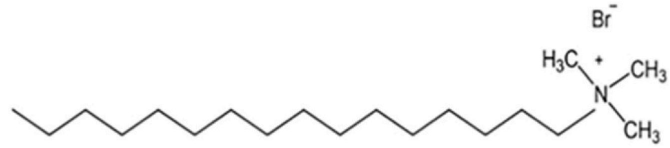

Fig. 19. CTAB chemical structure(Hossein Javadi and Fatemi, 2022).

Table 6
Different micromodel tests conducted (Hossein Javadi and Fatemi, 2022).

Test No.	Secondary injected solution	Tertiary injected solution
1	SW	SW + 1000 ppm (1000 mg/L) CTAB
2	10dSW	10dSW +1000 ppm CTAB
3	2cSW	2cSW + 1000 ppm CTAB
4	SW + 1000 ppm CTAB	–
5	10dSW +1000 ppm CTAB	–
6	2cSW + 1000 ppm CTAB	–

SW: Sea Water; d; Diluted: c; Concentrated.

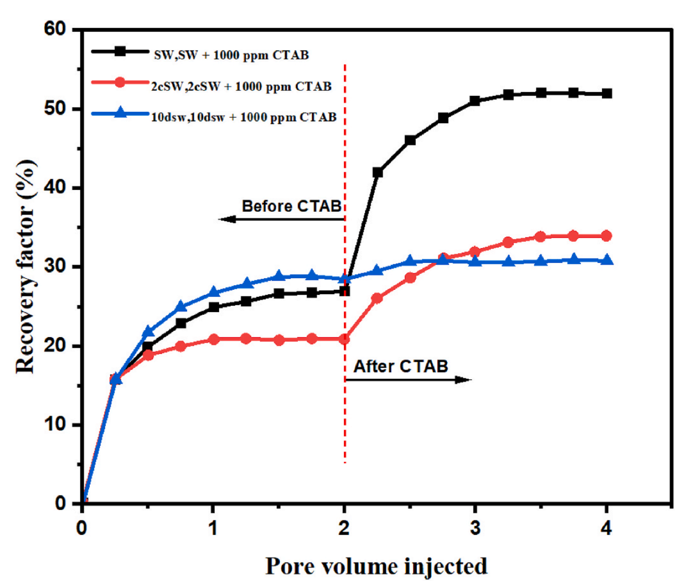

Fig. 20. Recovery factor increases during tertiary hybrid LSWF (Hossein Javadi and Fatemi, 2022).

after LSASF application which boosts oil recovery. Furthermore, the reactive transport model confirmed that diluting formation water causes the reduction of most reactive kaolinite clay edges minerals Si–O — and Al–O, which clarifies the reasons behind the increase in oil recovery.

Teklu (2015) experimented and simulated oil recovery increase using low-salinity water alternating carbon dioxide (LS-WACO_2) in low-permeability carbonate core samples with crude oil collected from the Middle East. Contact angle, IFT, and minimum miscibility pressure (MMP) were observed for wettability alteration. The results revealed that low salinity water increased oil recovery; however, after the injection of CO_2 gas, the oil recovery increased more, as shown in Fig. 22. Further, it was reported that CO_2 gas injected activated more wettability alteration to water wet. However, it was recommended that for LS-WACO_2 to be applied in low permeability reservoirs, hydraulic fracturing, and soaking are necessary to enhance the formation's permeability for easy flow of injected fluid and produced fluid towards the wellbore. Thus, it was concluded that LS-WACO_2 helps to clean natural and fractured formation matrix, viscosity reduction, and oil swelling. For simulation, Implicit in pressure Explicit in composition and saturation approach (IMPECS) was used in his study in which experimental results matched the simulation results.

Shabib-Asl et al. (2019) investigated the effectiveness of Low Salinity Water Assisted Foam flooding (LSWAF) on increasing oil recovery by using different salts and two crude oils in the laboratory for Berea sandstone reservoirs. Two crude oils were differentiated by Total Base Number (TBN) and Total Acid Number (TAN), which were called crude oil A and B, respectively. Salts used in the experiment were KCl, $MgCl_2$, $CaCl_2$, and NaCl.It was revealed that more cumulative oil was produced when KCl with 500 ppm concentration was used over other salinities in both types of crude oil. After the foam injection, the cumulative oil increased, as shown in Figs. 23 and 24. Furthermore, they proposed a new mechanism for hybrids LSWF on the ability to change wettability, i.e., Multicomponent Ion Exchange-Reactivity Series (MIE-RS), which states that "replacement of the divalent cations follows the reactivity series, $K^+ > Na^+ > Ca^{2+} > Mg^{2+}$". KCl at 500 ppm concentration changed the wettability of both types of crude oils, followed by NaCl, $MgCl_2$, $CaCl_2$, mixed composition, and FW. However, it was recommended that more laboratory studies are needed to support MIE-RS mechanisms, especially for carbonate reservoirs.

Piñerez Torrijos et al. (2018) experimented the effects of the hybrid EOR technique by using g low salinity (LS) Smart Water injection with polymer (P) injection in a sandstone formation. Their experiments were based on two parts which are secondary and tertiary recovery modes. In

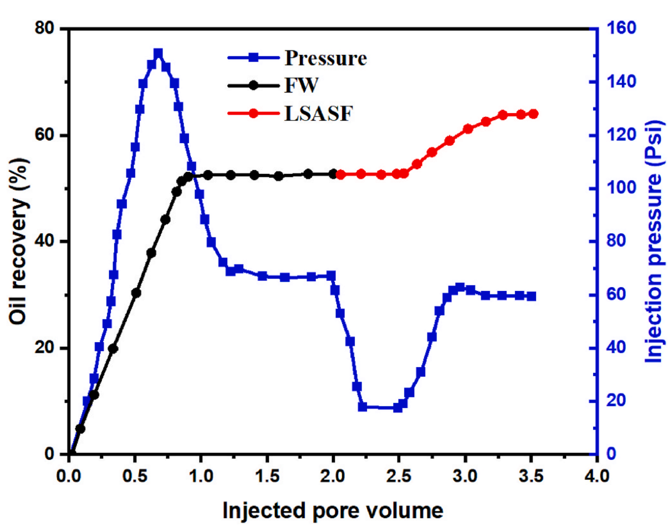

Fig. 21. Oil recovery versus injected pore volume for brine having less than 4887.5 ppm (Al-Saedi et al., 2020).

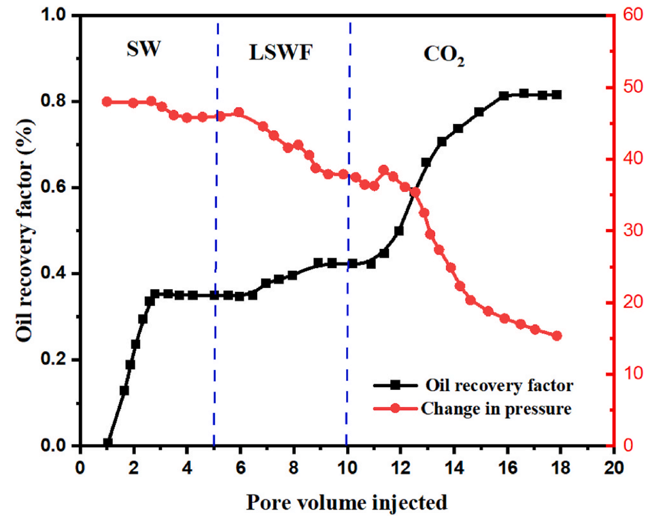

Fig. 22. Recovery factor versus pore volume injected(Teklu, 2015).

secondary recovery injection, it was found that salinity injection (SI) with formation water (FW) produced 33% of OOIP with no core wettability change, FW injection alone produced 40% of OOIP, SI produced 44% of OOIP, and hybrid LSPF produced 64% of OOIP after one pore volume injected. In tertiary recovery experiments, using SI, after FW, produced 5% more than secondary, indicating wettability changes by salinity water injection, and hybrid LSPF gave 86% of OOIP after low salinity injection. However, the performance of LSPF depends on the injection rate. A few selected studies on hybrid LSWF are shown in Table 7.

5.1. Challenges associated with hybrid LSWF application

1. Hybrid LSWF especially chemical based can not be applied in harsh conditions, especially in carbonate reservoirs, due to its low permeability and heterogeneity properties. For instance, LSPF can not be applied in high-pressure-high-temperature (HPHT) reservoirs, high salinity, and reservoirs with a high concentration of divalent ions (Kumar et al., 2016a; Lee and Lee, 2019). In addition, LSPF cannot be applied in reservoirs with high contents of CO_2 and H_2S

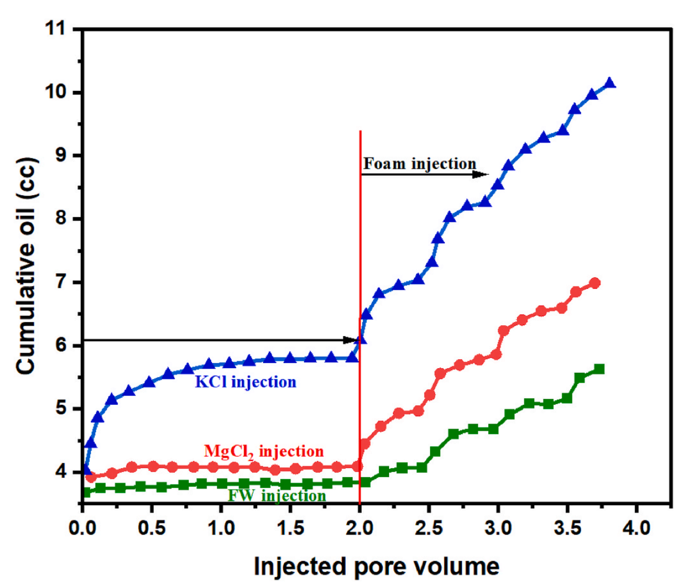

Fig. 23. Cumulative oil produced vs. injected pore volume for crude oil type A (Shabib-Asl et al., 2019).

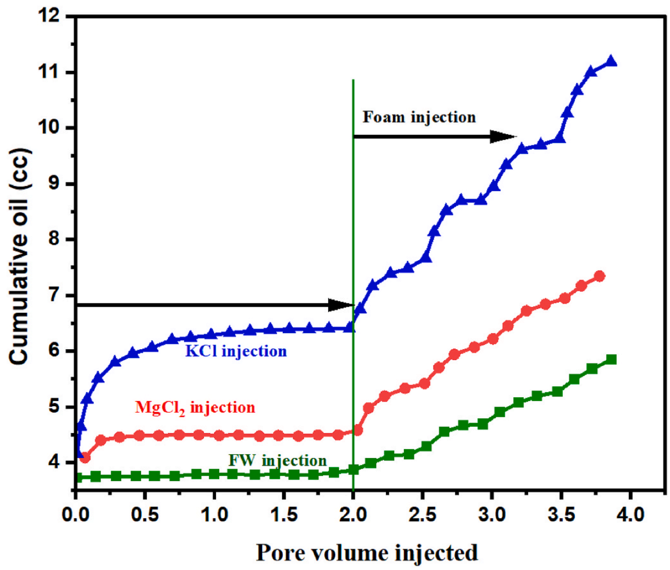

Fig. 24. Cumulative oil produced vs. injected pore volume for crude oil type B (Shabib-Asl et al., 2019).

(acidic conditions) because these components lower formation water pH, which makes LSPF ineffective by increasing polymer adsorption capacity to the rock surface(Brantson et al., 2020a; Samsuri, 2019).

2. Hybrid gas LSWF depend on the initial wettability of the reservoir, i.e., hybrid gas LSWF do not work out on water wet reservoirs, especially on sandstone reservoirs, because the role of LSWF is to change the wettability to water wet, which is already water wet instead salting-out effects dominate the production mechanism of hybrid gas LSWF. In addition, hybrid gas LSWF does not work on sandstone reservoirs with no clay(Lee et al., 2019a; Samsuri, 2019).
3. Similarly, hybrid polymer LSWF does not work for oil wet reservoirs because oil wet reservoir rock, such as rocks in carbonate reservoirs, are usually positively charged. The retention of hybrid polymer in LSWF could be considerable in positively charged surface. While it operates efficiently in sandstone reservoirs with water-wet properties, because the negatively charged rock surface in sandstone reservoirs could effectively reduce the hybrid polymer (also negatively charged) retention in the formation. Furthermore, hybrid polymer LSWF should be applied when the reservoir water cut is less or equal to 75% to improve oil recovery (Brantson et al., 2020a; Lee et al., 2018).
4. Also, nanoparticles are unstable at low salinity environments, so when designing hybrid nanoparticles, LSWF nanoparticle stability conditions should be carefully considered to improve oil recovery (Han et al., 2022; Pourafshary and Moradpour, 2019).
5. Another big challenge of hybrid LSWF is the high cost of chemicals such as polymer, surfactants, alkaline, etc., which are not available easily to the field site compared to low brine, which can be processed in the field by desalinating seawater. In contrast, chemicals need to be transported from different parts of the world, raising the cost of operations. So, the economic analysis must be conducted before implementing hybrid LSWF to the field scale to avoid financial loss (Pourafshary and Moradpour, 2019; Samsuri, 2019).

This section of the paper briefly demonstrated the potentiality of combining LSWF and other EOR techniques, such as chemical, thermal, or gas-based techniques. Hybrid EOR alleviates some challenges, such as environmental, economic, and operational issues, that individual methods face. Experiments, some modeling and simulation, and some pilot test studies have proved the potentiality of hybrid LSWF in increasing oil recovery factor by changing the oil wettability towards water wet as the main driving mechanism for LSWF and other mechanisms which destabilize the fluid properties(Lee et al., 2019a). Hybrid LSWF has proved to increase the oil recovery factor up to 30% of OOIP (Pourafshary and Moradpour, 2019). When combined with LSWF, thermal oil recovery improves oil mobility by lowering the IFT of oil, which helps in recovering more oil after detachment from the rock surface by LSWF(Lee and Lee, 2019). Also, when surfactants combined with LSWF decrease the IFT, thus lowering capillary pressure between oil and water, improving micro sweep efficiency after detachments of oil by LSWF(Javadi and Fatemi, 2022; Samanova, 2021; Shakeel et al., 2022). Further, the function of polymers in hybrid LSWF is to increase water viscosity which lowers the mobility ratio to less than one, thus helping to recover more oil after wettability alteration by LSWF. In addition, nanoparticles, especially SiO_2 in hybrid LSWF, assists in wettability alteration towards water wet as LSWF because it adsorbs easily on the rock surface, in situ emulsification, IFT reduction, and improving mobility ratio(Jin et al., 2022; Pourafshary and Moradpour, 2019). Lastly, gas injected (CO_2) in hybrids LSWF helps to change the waterfront of injected water, which helps in contacting unswept areas due to its minimum miscibility pressure and lowering free gas, which would come in contact with oil, thus improving oil mobility. Also, CO_2 reduces oil viscosity after swelling(Lee et al., 2019a).

6. LSWF field applications

Despite several theories, laboratory experiments, modeling and simulations, single well chemical tracer tests (SWCTT), and pilot tests involving LSWF, there are still limited full-field applications. This is attributed to several uncertainties from LSWF driving mechanisms, failure in SWCTT, and pilot tests. Another challenge is limited offshore space to build complex desalination units to supply low salinity water, which is expensive to make a project economical. However, there is a bright future for LSWF because there are full-field applications in Russia. Some major oil fields where LSWF has been studied and implemented are explained in this section.

6.1. Clair oil field, UK

Clair oil field is the largest offshore oil field discovered in 1977, located in the United Kingdom Continental Shelf, bordered by Scotland 132 miles in the northern part and Shetland Island 35 miles in the western part, with an area coverage of 220 km^2. It consists of old tight red sandstones divided into lower and upper Clair groups with many faults and fractures, making production to be complex. It has over 6 billion barrels of OOIP(Wilson, 2014). It started to produce oil in 2005 with 26 production wells and 11 injector wells. The oil field is producing under conventional water flooding and is expected to produce until 2050. After successfully producing Clair phase one (Graben) for five years by conventional waterflooding, the operators were pushed to consider developing Clair phase two (Clair ridge) with the target to produce twice compared to Clair phase one OOIP. Mwakipunda et al. (2023b) summarize Clair ridge's reservoir characteristics as shown in Table 8.

During Clair's phase two developments, LSWF caught attention after successfully of several core flooding experiments showed an increase in oil recovery, as shown in Table 9, during secondary injection over HSWF and other EOR techniques. After successful experimental investigations, modeling and simulations were implemented. It was reported that 47 out of 48 reservoir types showed a positive response using low-salinity brines with an average increase in oil recovery factor of 14.5% (Robbana et al., 2012). It is the only oil field in the UK where LSWF has been investigated under BP as the main operator (Chen et al., 2021). These results pushed single-well chemical tracer tests (SWCTT) and pilot tests which could not be performed before sanction. So far, BP is continuing to critically investigate the full field application of LSWF in Clair ridge after the first oil produced in 2018. Due to low permeability with high

Table 7
Some of the experimental research on hybrid LSWF.

Author(s)	Formation type	Hybrid	Observations
Lee et al. (2019b).	Carbonates	LSPF	-After LSWF, followed by LSPF oil recovery factor increased from 3.8% to 12.3%, with MIE as the driving mechanism. -Furthermore, neutral injected water (pH = 7) with polymer with highly concentrated SO_4^{2-}, increased oil recovery factor. -Wettability change to water wet was monitored through contact angle measurements
Brantson et al. (2020b).	Carbonates	LSPF	-Oil recovery factor increased to 39% compared to 31% of HSPF,24% of LSWF, and 11% of the normal waterflood. -MIE was the main driving mechanism of wettability alteration.
Moradpour et al. (2021).	Carbonates	LSWAG	-Oil recovery factor increased by 25.5% of OOIP. -CO_2 was used as alternating gas -Emulsion formation, contact angle, and solubility tests were conducted to examine the driving mechanisms. -Dissolution of minerals was the main driving wettability change mechanism. -Emulsion formation and MIE contributed to the oil recovery factor.
Al-Abri et al. (2019).	Sandstones	LSWAG	-Increased oil recovery factor up 23% OOIP - CO_2 was used as alternating gas -Dissolution was the main driving mechanism for wettability alteration.
Kumar et al. (2016b).	Sandstones	LSWAG	-More than 65% of OOIP was produced - CO_2 was used as alternating gas -MIE was the main driving mechanism in wettability change
Ramanathan et al. (2016).	Sandstones	LSWAG	-Recovered 97.7% of OOIP compared to 76.1% of OOIP by HSWAG injection. -CO_2 was used as alternating gas -Contact angle was used to asses wettability alteration. -MIE was the main driving mechanism in wettability alteration.
Teklu et al. (2017).	Carbonates	$LSSCO_2$	-Oil recovery factor increased up to 25% compared to Low salinity injection. -Fluid microdispersion was the main driving mechanism in wettability change. - Contact angle was used to asses wettability alteration.
Phukan and Saha (2022).	Sandstones	LSSAG	- Oil recovery factor increased from 12.92% to 23.16% of OOIP. -Dissolution was the main driving mechanism in wettability alteration. -CO_2 was used as alternating gas. - Contact angle was used to asses wettability alteration.
Karabayanova et al. (2022).	Carbonates	LSHW	-Oil recovery factor increased to 65% and 55% at 50 °C and 70 °C. -MIE and mineral dissolution were the main driving mechanisms in wettability change. -Viscosity reduction also increased the oil recovery factor. –
Dang et al. (2016a).	Sandstones	LSWAG	-Increased oil recovered factor by 4.5%–9% OOIP -CO_2 was used as alternating gas. -MIE was the main driving mechanism in wettability alteration.
Al-Saedi et al. (2018).	Sandstones	LSASF	-Oil recovery factor was 70.6% of OOIP. -Wettability change was monitored through contact angle measurement, which revealed that the wettability changed to mixed water wet conditions.
Ebaga-Ololo and Chon (2018)	Sandstones	LSSF	-Oil recovery factor increase up to 93.34 of OOIP for heavy oil and 99.87% of OOIP for light oil. -Added salt concentration reduced the IFT between the fluids and changed the phase behaviour of fluids.

LSWAG: Low salinity water alternating gas; HSWAG: High salinity water alternating gas; LSPF: Low salinity polymer flooding; LSHW: Low salinity waterflooding; LSSAG: Low salinity surfactant alternating gas flooding; LSASF: Low salinity-alternating-steam flooding; LSSF: Low salinity surfactant flooding; OOIP: Oil original in place; $LSSCO_2$: Low salinity water surfactant carbon dioxide.

viscosity, hydraulic fracturing has a great potential to enhance oil recovery in the unexploited areas of the Clair oil field during LSWF.

6.2. Endicott oil field, USA

This field is located in Alaska's North slope, bounded by the Beaufort Sea in the North and the maritime border with Russia in the Western part, with 45 acres area coverage located at coordinates 70.3500° N, 147.9583° W. It has initial oil saturation of 95% (Adamson et al., 1991; Seccombe et al., 2010). It is an artificial island built in 1987 to facilitate hydrocarbon production, with the processed oil transported through a pipeline of 39 km to the mainland larger pipeline under BP and Hilcorp Alaska (Lager et al., 2011; Woidneck et al., 1987). Endicott oil field is producing using gas re-injection, seawater injection, and produced water injection with 11 million b/d of oil and 1 million b/d of natural gas liquids (NGL) with an average water cut of 94% and an average gas-oil ratio of 3000 scf/stb. More than 129 wells have been drilled. It has 88 active wells, of which 63 are production wells, and 25 are injection wells (Seccombe et al., 2010).

The porosity in the Endicott oil field is secondary porosity formed by the leaching of siderite. The Endicott oil field is divided into two major zones: upper and lower subzones. The upper subzones include K3B and K3C. The lower sub-zones, with average porosity, include K2A, K2B, and K3A. The average porosity and permeability of K2A and K2B are 1400 mD and 20%, respectively. K3A has an average porosity and permeability of 800 mD and 21%, respectively. The lower subzones are intended for LSWF(Maki, 1992; Seccombe et al., 2010).

After successful core flooding experiments, SWCTT (Table 10), and simulations results, in December 2007 pilot test was initiated in the

Table 8
Clair ridge reservoir characteristics (Mwakipunda et al., 2023b).

Parameters	Symbol	Value	Units
Formation properties			
Reservoir depth	D	1400	m, subsea
Oil water contact	OWC	–	m, subsea
Closure area	A	220	km^2
Net pay	h_n	–	m
Total pay	h_t	–	m
Permeability	k	70-119-7000	mD
Fluid properties			
Bubble point pressure	P_b	–	bara
Solution GOR	R_s	68	m^3/m^3
Oil gravity	ρ_0	24	degrees API
Formation volume factor	B_0	–	Res $vol/std\ vol$
Oil viscosity	μ_0	3.2	cP
Sulphur content	–	0.44	mol %
Reservoir			
Temperature	T_R	–	$^\circ C$
Initial pressure	P_i	244.7775	bara
Oil initial in place	OIIP	1.3	B m^3

Table 9
LSWF core flooding oil recovery increase over HSWF(Chen et al., 2021).

Source rock	Permeability (mD)	Oil recovery factor (%)
Clair main	25	9
Clair main	100	13.1

Endicott oil field using one production and one injection well. Its purpose was to determine the impacts of tertiary low-salinity brine on increasing oil recovery factor over high-salinity brine. The critical factors of pilot test design considerations are summarized in Table 11. The subzone K3A was selected for LSWF pilot tests because it has high clay contents, which contribute to oil recovery increase, and has underlying and overlying shales separating it from other wells to avoid well interferences. K3A has a thickness of 30–45 ft with two wells 1040 ft apart with a temperature of 99 °C. Afterpulse tests, two wells, 3–35 (L-36) as injector and 3–37 (L-35) as a producer, were selected because they have good inter-well communication. Fig. 25 shows the cross-section and structure map of sub-zone K3A. HSWF started on December 7, 2007, and production was noticed immediately and continued until a 95% water cut was reached. After that, on June 4, 2008, LSWF was initiated until October 5, 2008, with data collected and water cut measured after 5 min to notice the arrival of injected low salinity with observations in the increase in oil recovery.

The results revealed that, and oil rate increased, as shown in Fig. 26 (a), whereas the water cut reduced from 95% to 92%, as shown in Fig. 26 (b). In addition, modeling and simulation were conducted in which relative permeability curves were generated from the history matching using clay and water content data (Seccombe et al., 2010). The simulator revealed that the low salinity water injection matched the pilot test findings, and LSWF should be implemented successfully in full field scale operation in the Endicott oil field. The lesson learned from the Endicott oil field should be adopted and applied in matured oil reservoirs and pave the way for LSWF full-field applications. However, in 2014 BP announced the sale of its shares to Hilcorp Alaska for 5.6 billion US dollars, and in 2019, the deal was completed (Wood et al., 1991).

6.3. Pervomaiskoye field, Russia

This oil field is located in the central part of Russia (Tatarstan) and was discovered in 1958, saturated with light oil having 5.8 mPa s viscosity with a reservoir thickness of 30 m. The pay zone is made of sandstone and siltstone. It comprises five layers, four of which are saturated with oil and one at the bottom saturated with water. The formation thickness varies from 20 to 40 m, with a net pay thickness of 8–18 m. The layers are grouped into two horizons: The upper two layers (Kynovsky) and the Lower three layers (Pashiyski), which consist of the Devonian geological system. The fluids and rock properties of the Pervomaiskoye oil field are shown in Table 12 (Akhmetgareev and Khisamov, 2015; ХисаМов et al., 2020).

The oil field produced by natural pressure for seven years. Waterflooding started after primary energy depletion in 1966, with all injectors in the middle of the reservoir and aquifer zone. The wells were separated at a distance of 600–1500 m, with 80% of injected water taken from Karma river due to little produced water. Both high salinity and low salinity water were injected, and high salinity injection outperformed lower salinity, as shown in Fig. 27. Since 1991, the field has been under the fourth stage of development, with reservoir pressure decreasing to 360000 tons per year from 650000 tons per year and water cut increased from 89 to 94%. Up to 2015, 513 wells were drilled (Akhmetgareev and Khisamov, 2015).

Table 10
SWCTT results for Endicott oil field (Seccombe et al., 2008).

No.	Year	HSWF (S_{or}) %	LSWF (S_{or}) %	Difference (%)
1	1989	39	–	
2	2004	43	34	9
3	2005	42	25	17
4	2005	40	–	
5	2006	41	30	11

(S_{or}): Residual oil saturation.

Table 11
Consideration factors for pilot test design (Seccombe et al., 2010).

No.	Key design
1	Sub zones selection for flooding
2	Pair of wells selection
3	Water source selection for LSWF
4	Determine how low salinity water will be delivered from the source to the injection well
5	Develop the surveillance program
6	Repeatability and accurate measurements of oil production and water cut during production
7	Using numerical simulators and analytical calculations, anticipate the time, degree of response, and sensitivity.

In 2005 seven LSWF pilot tests were conducted for wells that initially were operated by HSWF, with each injector having 2 to 5 producer wells. As shown in Fig. 28, all seven pilot tests responded by increasing the oil recovery factor after LSWF. Also, the water cut decreased from 87% to 80%; the production rate increased from 2.1 to (2.5–3.1) tons/day, which confirms the effectiveness of LSWF over HSWF, whereas if HSWF continued production rate could be 1.5 tons/day. Additionally, water produced density decreased from (1.13–1.17) g/cm^3 to (1.04–1.08) g/cm^{3,} confirming that injected low salinity water has reached producer wells(Akhmetgareev and Khisamov, 2015). This shows that all HSWF injector wells can be converted to LSWF injectors to enhance oil production in the Pervomaiskoye oil field(Akhmetgareev and Khisamov, 2015).

6.4. Snorre oil field, Norway

Snorre oil field is one of the major fields in the southern part of the Norwegian Sea, 150 km from the Norwegian Continental Shelf (NCF), having undersaturated oil initially in place of 513 million standard cubic meters discovered in 1979, with the first oil produced in 1992 under Saga oil company (Mukherjee et al., 2020; Skrettingland et al., 2016). Up to 2011, three-quarters of oil was produced from the field. In 2010 the Saga was transferred to Equinor ASA. It is located in the Tampen area, latitude 61° 27′ 0″ N and longitude 2° 7′ 48″ E in a sea depth of 300–350 m. Snorre oil field is made up of two major formations: Statfjord formation and Lunde formation, with a range of wettability from mixed water wet to water wet formed during the Early Jurassic and Late Triassic. The formations are complex with heterogeneous strata fluvial sandstones with a dip angle of 6–8°. Other reservoir characteristics of the Snorre oil field are shown in Table 13 (Chen et al., 2022).

The first oil produced in 1992 was due to seawater injection as the main driving mechanism, and in 1996 switched to water-alternating gas injection. With ambitions of increasing oil recovery to more than 55%, various improved and enhanced oil recovery techniques have been tested and applied, including LSWF. Core flooding has been conducted under reservoir temperature in both formations to investigate low salinity water potentiality in increasing oil recovery. The range of salinity concentration was 375–3500 ppm. However, in most of the experiments, the salinity concentration used was 500–2000 ppm. In all experiments, high salinity water was injected first until no oil was produced, followed by low salinity injection. The injection rate during experiments was 8 mL/h. According to the reports, core flooding experiments with low salinity water increased oil recovery from 0.9 to 2.6% of OOIP in the Statfjord formation, while no significant response was shown for Lunde formations. After the core flooding success, several

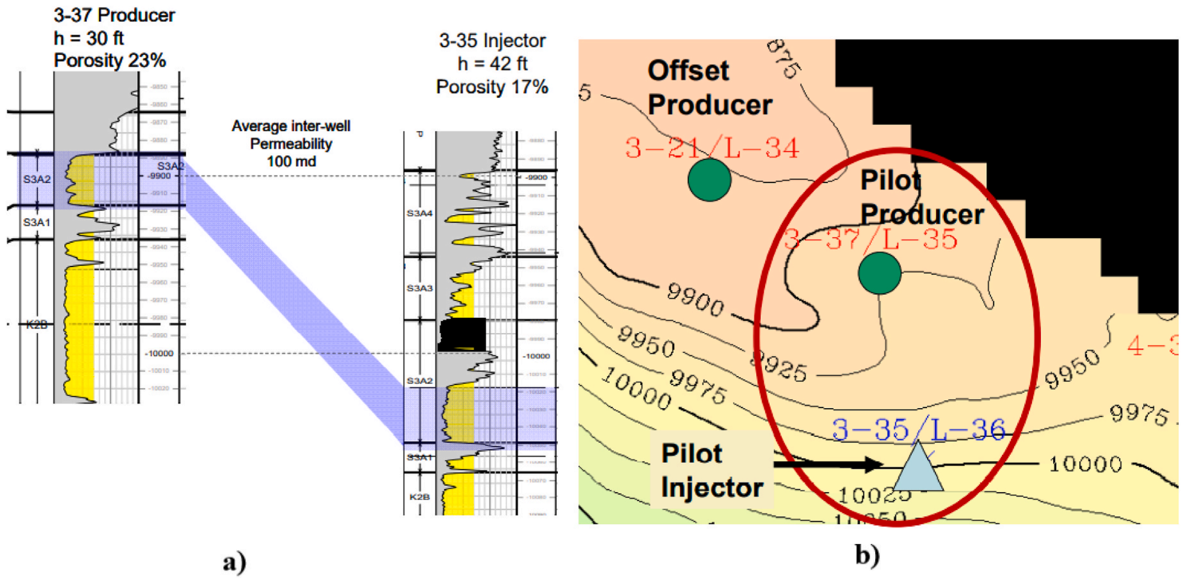

Fig. 25. Sub zones K3A a) Cross section b) Map structure (Seccombe et al., 2010).

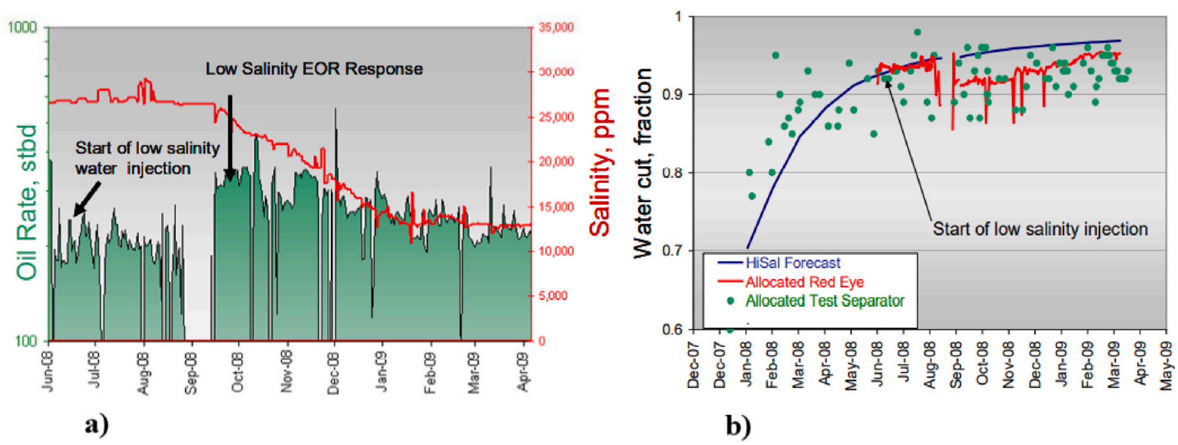

Fig. 26. a) Oil rate increase after LSWF b) Water cut decrease after LSWF (Seccombe et al., 2010).

Table 12
Pervomaiskoye field properties (Akhmetgareev and Khisamov, 2015).

Parameter	Value	Units
Formation properties		
Top depth	1660	m
Average net pay thickness	8	m
Average formation thickness	30	m
Sandstone relative layers thickness	0.484	m
Reservoir properties		
Temperature	30	°C
Pressure	16.6	MPa
Fluid properties		
Gas oil ratio	39	$m^3/tons$
Bubble point pressure	9.2	MPa
Oil density (In-situ)	845	Kg/m^3
Surface oil density	873	Kg/m^3
Formation volume factor	1.105	bbl/STB
Oil viscosity (In-situ)	5.8	mPa.s
Water density (In-situ)	1176	Kg/m^3
Water viscosity (In-situ)	1.787	mPa
Core floods displacement efficiency	0.652	–
Water oil contact	−1470	m

SWCTT test was conducted. The results matched the core flooding findings. However, during the pilot test, the results did not match the previous core flooding and SWCTT findings. It was observed that the oil recovery increase was very low or not observed. The reason for this is the initial wettability condition of the Snorre field (water-wet); indeed, the injected sea water during secondary recovery responded efficiently (Chen et al., 2022). Thus, low tertiary salinity can increase oil recovery only at a marginal cost. This study shows the importance of the initial wettability of the reservoirs in LSWF (Chen et al., 2021; Sheng, 2014; Skrettingland et al., 2011). Hence, it was concluded that LSWF potentiality at Snorre field is low, with its life span predicted to be the 2040s.

7. Formation damage effects during low salinity waterflooding

Formation damage is one of the major problems in the oil and gas industry, either near the wellbore or in the reservoir, caused by fines migrations, thus reducing oil recovery(Hussain et al., 2014; Ngata et al., 2022a; Schembre and Kovscek, 2005; Yu et al., 2018, 2019). However, during LSWF, fines migrations have been shown to increase oil recovery by blocking the swept areas and causing the diversion of low-salinity injected brine to mobilize residual oil in unswept areas (Ligeiro et al., 2022; Song and Kovscek, 2016; Tang and Morrow, 1999a; Yuan and Moghanloo, 2018; Zeinijahromi et al., 2011, 2015, 2016). After the

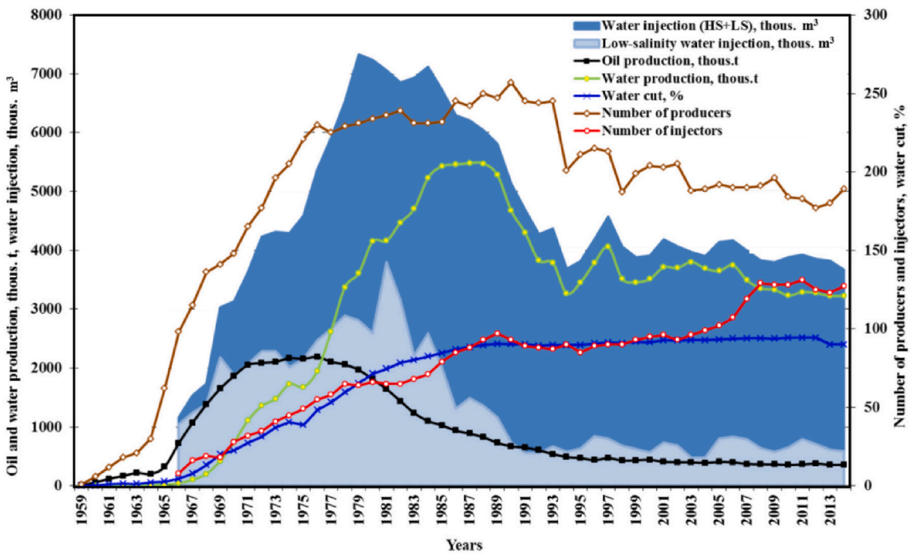

Fig. 27. Production trend for the Pervomaiskoye field (Akhmetgareev and Khisamov, 2015).

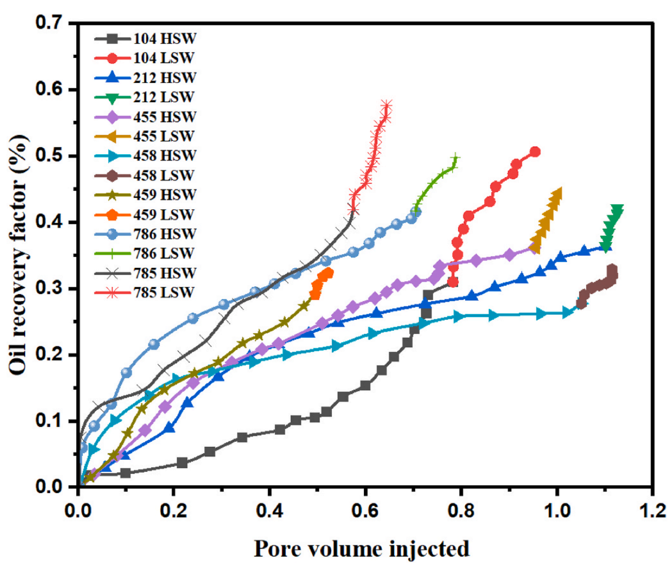

Fig. 28. Oil recovery factor versus pore volume injected (Akhmetgareev and Khisamov, 2015).

Table 13
Snorre reservoir parameters (Skrettingland et al., 2011).

Reservoir parameter	Value	Unit
Maximum gross thickness	1000	m
Net/gross - thickness	0.45	–
Porosity	14–32	%
Permeability	100–4000	mD
Clay	5–35	%
Temperature	90	°C
Initial pressure	383	bar

micromodel experiment, Mehdizad et al. (2022b) observed that formation damage occurs during LSWF in the reservoir. They divided it into three stages: (i) Throat blocking stage, caused by clay migration and swelling during sodium bentonite injection, which blocked some throats, and the diversion of injected low salinity water, which helps sweep residual oil trapped in unswept areas. Fig. 29 (a) shows an unblocked throat before brine injection, which is partially open to allow fluid to flow. After low salinity water injection starts from left to right and passes through that throat, damage (throat blocking) starts due to clay swelling and migration, as shown in Fig. 29 (b). As the injection continued, the throat was blocked due to clay accumulation and swelling, as shown in Fig. 29 (c), and a throat was blocked. However, the injected brine always diverts to find another path to flow either below or above the blocked throat. Hence, injected brine helps to mobilize residual oil saturation in unswept areas and sweep toward the production well, as shown in Fig. 29 (c). (ii) Reduction of pore throat diameter; this occurs before throat blockage after clays are swollen to a great extent to reduce the throat diameter (permeability). Fig. 30 shows how this occurs from micromodel tests whereby after low salinity brine injection started, the fluid distribution change occurred due to clay/brine/oil interactions as shown in the right-hand side of Fig. 30, which is different from the left-hand side of Fig. 30 before the low salinity brine injection. However, due to high-pressure buildup caused by brine injection, the pore throat diameter is reduced due to clay migration and swelling. (iii) Throat unblocking, this was observed during continuous LSWF, whereby some blocked throats during fluid diversion were unblocked. From Fig. 31 (a) shows a blocked throat which prevents low salinity brine flowing from the upper to the bottom part to sweep oil in the right-hand side, however as low salinity brine injection continues, the unblocking process starts, as shown in Fig. 31 (b) due to clay migration forces. After that, in Fig. 31 (c), the blocked throat is completely open, allowing low salinity brine to flow towards the right side to sweep oil in uninvaded zones. However, Mahmoud et al. (2017) reported that chemicals from added cations like calcium sulfate always precipitate, which causes formation damage during injection, thus reducing the injectivity rate. The solution adds chelating agents like Ethylenediaminetetraaacetic acid (EDTA), Diethylenetriamene pentaacetate (DTPA), Methylglycindiessigsaure (MGDA), Methylglycinediacetic acid (HEIDA), etc., and nanoparticles during LSWF, which must be used at high pH to prevent corrosion problems (Mahmoud et al., 2017; Ngata et al., 2022b).

In addition, Mehdizad et al. (2022a) did a micromodel test on the influence of brine contents and compositions on formation damage during LSWF because its affects clay swelling and migration, which causes a reduction of porosity and permeability, which results to lower oil recovery. In their experiments, it was revealed that salt with a small hydrate radius helps to reduce formation damage during LSWF. For instance, KCl having a small hydrate radius and divalent cations, reduced porosity by 2.8%, while $CaCl_2$ alone reduced porosity by 7%. This shows that KCl controlled clay swelling and migration compared to $CaCl_2$.

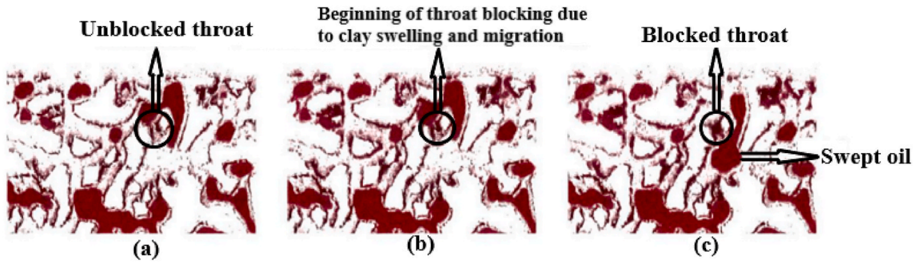

Fig. 29. Throat blocking stages during LSWF(Mehdizad et al., 2022b).

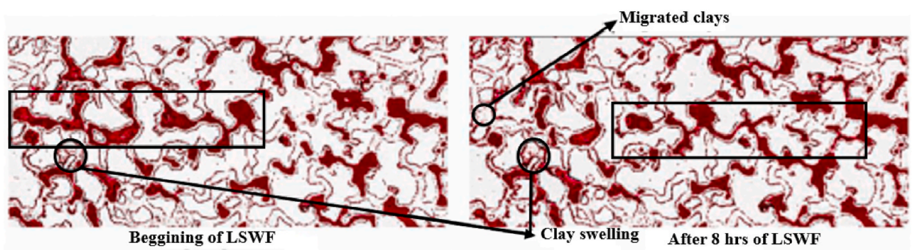

Fig. 30. Reduction of pore throat and diameter during LSWF(Mehdizad et al., 2022b).

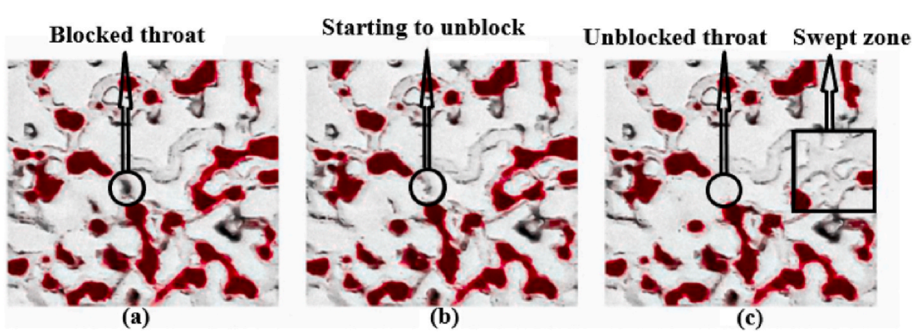

Fig. 31. Throat unblocking during LSWF(Mehdizad et al., 2022b).

8. Challenges encountered during LSWF

LSWF increases oil recovery by changing rock surface wettability, lowering oil-water interfacial tension, and deploying particles and oil droplets. These techniques can boost water flood sweeping and displacement efficiency, increasing oil production and reducing water cut. However, optimizing its performance and minimizing potential problems requires rigorous design, monitoring, and evaluation. The challenges encountered during LSWF include: Scaling; injecting low salinity water into the reservoir cause scaling problems in the wellbore and other facilities, resulting in low production rate and reducing cumulative oil production(Cabrera S and Samaniego, 2022; Khandoozi et al., 2020). Reservoir heterogeneity; when the reservoir is heterogeneous, it causes uneven distribution of injected low salinity water, resulting in low oil recovery(Al-Ibadi et al., 2020; Ladipo et al., 2022; Wood and Yuan, 2018). Also, clay swelling; because the reservoirs contain clay minerals after LSWF into the reservoirs causes clay swelling, which results in permeability reduction and affects oil production(Barnaji et al., 2016; Bhui and Desai, 2015). Further, the lack of data, in understating LSWF mechanisms and its effects on increasing oil recovery requires larger data sets that need to be collected in the particular oil field(Takeya et al., 2019; Tatar et al., 2021). Furthermore, implementing LSWF project in the real field is very expensive and differs from one field to another. However, it depends on the reservoir's size and complexity (Alvi and Qureshi, 2023; Saw et al., 2022).

Another challenge is health and safety issues; because LSWF involves using larger amounts of water enriched with several chemicals when handled improperly, it poses health and safety issues to workers(Aladasani, 2012). Also, regulatory requirements; to implement LSWF require permission from local authorities which takes a long time and is costly to acquire the license. This increases the complexity of the project (Abbas et al., 2020; Al-Ibadi et al., 2019a). Furthermore, environmental issues; LSWF needs a large amount of processed water to be injected into the reservoir, so this injected water can contaminate the aquifer zone when leakage occurs during injections. In addition, larger water drainage from the source, if not the sea, can result in small scale earthquakes (Butt et al., 2022; Hien et al., 2021). Further, water quality; water used for LSWF requires fewer impurities, which means water needs to be processed for LSWF purpose; otherwise, it will affect the processes and results in low oil recovery(Chen et al., 2021; Dwivedi et al., 2023; Shi et al., 2021). Furthermore, salt dispersion and brine mixing, after low salinity water is injected in the reservoir, it mixes with high salinity water (resident water), which results in the development of a mixing zone (salt dispersion) with high salinity compared to injected brine which grows continuously from the injection well towards a production well. This increase in the salinity of the water front reduces LSWF efficiency. To minimize this problem, the optimal volume of LSW to be injected to avoid salt dispersion and brine mixing should be determined (Al-Ibadi et al., 2019b; Darvish Sarvestani et al., 2021, 2022; Jerauld et al., 2008; Ladipo et al., 2020). On the other hand, adding other chemicals to LSW has been suggested to reduce this problem, as discussed by (Darvish Sarvestani et al., 2021, 2022).

9. Research gaps and future work

LSWF has great potential to increase oil recovery in the mature oil field to meet future global energy demand. However, many conducted researches contradict each other about the mechanisms behind either rock-to-fluid interactions, fluid-to-fluid interactions, or rock-fluid-fluid interaction (in carbonate reservoirs) contributing to wettability change during LSWF. Noted areas that need more investigations in future research works are outlined below:

1. In most LSWF simulation models, capillary pressure change effects are neglected, which is important in constructing the simulation flow models. More studies are suggested to consider capillary pressure changes to reflect field reality.
2. Most experiments focused on determining how wettability changes lead to oil production. However, it is unclear how changes in the wetting phase result in oil production during LSWF due to lack of several relatives of pore scale observations. Some models rely on clay's ionic exchange, which is insufficient for clay-free rock.
3. LSWF current simulation models are based on geochemical interactions; however, the fluid-fluid interaction has been neglected. More research on the fluid-fluid interaction influence on oil recovery needs to be conducted.
4. Osmotic effect is believed to be one of the LSWF mechanisms in enhancing oil recovery through the osmosis process. However, how it contributes to wettability alterations is not clear. A critical investigation is needed to confirm how osmosis alters wettability after LSWF using spontaneous-imbibitions tests or other methods.
5. The detachments of naphthenic acids (NAs) from crude after interactions with brine significantly reduce crude oil pH, possibly changing wettability from oil-wet to mixed wet or water wet. This area needs more scientific investigation in the future because most established surface complexation models made several assumptions and are not valid in higher ionic strength (Bonto et al., 2019; Miadonye et al., 2023).

10. Conclusions and recommendations

This paper presented the overview of LSWF and the general full-field applications to secure future energy demand. The mechanisms and recent progress have been investigated and analyzed. The research gaps and future works have been discussed. LWSF has been found to have great potential to increase oil recovery in some of the matured oil fields. The potentiality of hybrid LSWF has been discussed. Despite showing a bright future in recovering residual oil saturations, the mechanisms behind LSWF are unclear and still under research due to inconsistent results. The following points have been drawn from this review paper:

1. Reservoir mineral surfaces affect wettability changes and an increase in oil recovery during LSWF. It was found that a sand reservoir with kaolinite is more suitable for LSWF than sandstone with illite because kaolinite has a higher carboxylate adsorption capacity and more surface edges than illite.
2. Fluid-fluid interactions, especially oil-injected brine microdispersion formation, have recently emerged as another LSWF driving mechanism over rock-to-fluid interactions. It was added that clay is not an influencing factor for LSWF. It is recommended to have more pore scale investigations about microdispersion formation as it emerged as the driving mechanism of wettability alteration.
3. Low salinity with a concentration range of 1400–5000 ppm in injected water is recommended to increase oil recovery in sandstone-matured oil reservoirs. In carbonate rocks, salinity should be less than 10000 ppm.
4. Despite a smaller number of research conducted in carbonate oil reservoirs for LSWF compared to sandstone reservoirs, the appropriate mechanisms proposed are due to its nature of having fractures and multiple porosities.
5. Formation damage during LSWF seems to increase oil recovery instead of decreasing through blocking the swept areas after the fines migration process, which diverts injected low salinity brine to mobilize residual oil in unswept zones and thus flow towards the production wellbore.
6. Hybrid LSWF has shown great success over LSWF in increasing oil recovery. However, due to additional cost of chemicals could make a hybrid LSWF challenging economically in the full-field application. It is recommended to be tested in areas where LSWF has shown failure, like the Snorre oil field associated with economic evaluations.
7. LSWF can be applied at any stage of hydrocarbon oil production because it is used in improved oil recovery (IOR) and enhanced oil recovery (EOR). Also, it has less cost, a low carbon dioxide footprint, less scaling and souring, less environmental impact, etc., compared to other secondary and tertiary recovery techniques.
8. LSWF is more favorable to weak oil wet and mixed wet reservoirs because strong oil wet or water wet adheres more to the rock surface and thus is difficult to detach by changing brine composition.
9. For carbonate and sandstone reservoirs, the oil recovery increases due to LSWF is approximately 6–10% and 7–20%, respectively, for tertiary recovery stage.
10. Among the many simulators evaluated for LSWF are CMG, UTCHEM, and SOLMINEQ.88, IPHREEQC, TOUGHREACT, Computer modeling group (CMG), Geochemist's Workbench, Schlumberger Eclipse, UTCHEM-IPHREEQC, KGEOFLOW, machine learning, etc., taking into account different factors during LSWF to reflect the field reality. CMG and UTCHEM-IPHREEQC better predicted the oil recovery factor than other simulators. Developing a simulator that considers all the proposed LSWF mechanisms for better prediction toward field application is recommended.

Declaration of competing interest

The authors declare that there is no conflict of interest.

Data availability

No data was used for the research described in the article.

Acknowledgments

The Authors thank Chinese Scholarship Council for their support

Appendix A

Table A1
The increase of RF by LSWF in different formations and salinity.

No.	Source	Test scale	Formation type	Temperature (°C)	Salt concentration (ppm)	Oil recovery factor
1	Chávez-Miyauch et al. (2020).	Core scale	Sandstones	Room temperature 20	3550	53%–66% OOIP
2	Loahardjo et al. (2007).	Core scale	Sandstones	60	350	17% OOIP
3	Winoto et al. (2012).	Core scale	Carbonates	60	1750	39%–41% OOIP
4	Bhicajee and Romero-Zerón (2021).	Core scale	Sandstones	Room temperature 25	8410	Increased by 20% OOIP
5	Vledder et al. (2010).	Field scale	Sandstones	–	2200	10%–15% OOIP
6	Yousef et al. (2011).	Core scale	Carbonates	Reservoir temperature 100	350	74%–94% OOIP
7	Webb et al. (2004).	Field scale	Sandstones	–	3000	20%–50% reduction in residual oil saturation
8	Torrijos et al. (2018).	Core scale	Sandstones	60	1000	Increased by 38% of OOIP
9	Hien et al. (2021).	Simulation	Sandstones	Reservoir temperature 93	1000	Increased by 2.9% of OOIP
10	McGuire et al. (2005b).	Field scale	Sandstones	71.11	1500	6%–12% of OOIP
11	Austad et al. (2010a).	Core scale	Sandstones	40	1500	40–75% of OOIP
12	Pu et al. (2010).	Core scale	Sandstones with anhydrite cement	60	1538	5%–8% OOIP
13	Pu et al. (2010).	Core scale	Dolomites	60	1538	5%–8% OOIP
14	Austad et al. (2012).	Core scale	Carbonates	110	100	2%–5% OOIP
15	Al-Harrasi et al. (2012).	Core scale	Carbonates	70	97225	16%–21% OOIP
16	AlHammadi et al. (2018).	Core scale	Carbonates	Room temperature 25 and 60	<10000	Increased by 6%
17	Masalmeh et al. (2019).	Core scale	Carbonates	90	480	Increased by 7%
18	Saw and Mandal (2020).	Core scale	Carbonates	90	1750	20% OOIP
19	Bartels et al. (2016)	Pore scale	Sandstones	60	12897	Increased by 3%
20	Siadatifar et al. (2021)	Pore scale	Sandstones	25	3500	Increased by 2%
21	Siadatifar et al. (2021)	Pore scale	Limestones	25	3500	Increased by 3%
22	Amirian et al. (2017)	Pore scale	Clay	80	<6000	-Increased by 10% in the absence of clay. -Increased by 15% in the presence of clay.

OOIP: Original oil in place; EOR: Enhanced oil recovery.

References

Abbas, S.R., et al., 2020. Impact analysis of large-scale wind farms integration in weak transmission grid from technical perspectives. Energies 13 (20), 5513.
Adamson, G., Hellman, H., Metzger, R., 1991. Design and Implementation of the First Arctic Offshore Waterflood, Endicott Field, Alaska. SPE Western Regional Meeting, OnePetro.
Afifi, H.R., et al., 2021. A comprehensive review on critical affecting parameters on foam stability and recent advancements for foam-based EOR scenario. J. Mol. Liq., 116808
Agzamov, A., et al., 2023. On the degree of influence of waterflooding on the oil recovery factor from productive formations of high-viscosity reservoirs X, represented by terrigenous reservoirs. Kompleksnoe Ispolzovanie Mineralnogo Syra 326 (3), 50–58.
Akbarifard, M.G., Azdarpour, A., Arab Aboosadi, Z., Honarvar, B., Nabipour, M., 2020. Investigation of the Impact of Polymer Gels on Water and Gas Production in Homa Gas Field Using Well and Reservoir Modeling. Energy Sources, Part A: Recovery, Utilization, and Environmental Effects, pp. 1–14.
Akhmetgareev, V., Khisamov, R., 2015. 40 Years of Low-Salinity Waterflooding in Pervomaiskoye Field, Russia: Incremental Oil. SPE European Formation Damage Conference and Exhibition.
Al-Abri, H., Pourafshary, P., Mosavat, N., Al Hadhrami, H., 2019. A study of the performance of the LSWA CO2 EOR technique on improvement of oil recovery in sandstones. Petroleum 5 (1), 58–66.
Al-Attar, H.H., Mahmoud, M.Y., Zekri, A.Y., Almehaideb, R., Ghannam, M., 2013. Low-salinity flooding in a selected carbonate reservoir: experimental approach. J. Pet. Explor. Prod. Technol. 3 (2), 139–149.
Al-Harrasi, A.S., Al-Maamari, R.S., Masalmeh, S., 2012. Laboratory Investigation of Low Salinity Waterflooding for Carbonate Reservoirs. Abu Dhabi International Petroleum Conference and Exhibition.
Al-Ibadi, H., Stephen, K., Mackay, E., 2019a. Novel observations of salinity transport in low-salinity waterflooding. SPE J. 24 (3), 1108–1122.
Al-Ibadi, H., Stephen, K.D., Mackay, E., 2019b. Insights into the fractional flow of low salinity water flooding in the light of solute dispersion and effective salinity interactions. J. Petrol. Sci. Eng. 174, 1236–1248.
Al-Ibadi, H., Stephen, K., Mackay, E., 2020. Heterogeneity Effects on Low Salinity Water Flooding. SPE Europec, OnePetro.
Al-Saedi, H.N., Flori, R.E., Mortadha, A., 2018. Coupling Low Salinity Water Flooding and Steam Flooding for Heavy Oil in Sandstone Reservoirs; Low Salinity-Alternating-Steam Flooding LSASF: A Novel EOR Technique. Abu Dhabi International Petroleum Exhibition & Conference.
Al-Saedi, H.N., Flori, R.E., Al-Bazzaz, W., 2020. Will coupling low salinity water and steam flooding for heavy oil affect the rock properties of sandstone reservoirs? An experimental and simulation study. J. Mol. Liq. 306, 112866.
Al-Sarihi, A., et al., 2018. Effects of fines migration on residual oil during low-salinity waterflooding. Energy Fuel. 32 (8), 8296–8309.
Al-Shalabi, E.W., Sepehrnoori, K., 2016. A comprehensive review of low salinity/engineered water injections and their applications in sandstone and carbonate rocks. J. Petrol. Sci. Eng. 139, 137–161.
Aladasani, A., 2012. Updated EOR Screening Criteria and Modeling the Impacts of Water Salinity Changes on Oil Recovery. Missouri University of Science and Technology.
Alhammadi, M., Mahzari, P., Sohrabi, M., 2017. Experimental Investigation of the Underlying Mechanism behind Improved Oil Recovery by Low Salinity Water Injection in Carbonate Reservoir Rocks. Abu Dhabi International Petroleum Exhibition & Conference.
AlHammadi, M., Mahzari, P., Sohrabi, M., 2018. Fundamental investigation of underlying mechanisms behind improved oil recovery by low salinity water injection in carbonate rocks. Fuel 220, 345–357.
Alhuraishawy, A.K., Bai, B., Wei, M., Geng, J., Pu, J., 2018. Mineral dissolution and fine migration effect on oil recovery factor by low-salinity water flooding in low-permeability sandstone reservoir. Fuel 220, 898–907.
Aljaberi, A., Sohrabi, M., 2019. A New Approach to Simulate Low Salinity Water Flooding in Carbonate Reservoir, SPE Middle East Oil and Gas Show and Conference.
Aljaberi, A., Aghabozorgi, S., Sohrabi, M., 2022a. A Universal Method for Predicting the Relative Permeability Data of Low Salinity Injection. SPE EuropEC - Europe Energy Conference featured at the 83rd EAGE Annual Conference & Exhibition.
Aljaberi, A., Aghabozorgi, S., Sohrabi, M., 2022b. A Universal Method for Predicting the Relative Permeability Data of Low Salinity Injection. SPE EuropEC-Europe Energy Conference featured at the 83rd EAGE Annual Conference & Exhibition. OnePetro.
Alvi, F., Qureshi, H.A., 2023. Technical and economic feasibility assessment of low and high salinity water flooding: a simulation-based approach. Int. J. Energy Environ. Eng. 1–16.
Amirian, T., Haghighi, M., Mostaghimi, P., 2017. Pore scale visualization of low salinity water flooding as an enhanced oil recovery method. Energy Fuel. 31 (12), 13133–13143.
Anderson, W.G., 1986. Wettability literature survey-part 1: rock/oil/brine interactions and the effects of core handling on wettability. J. Petrol. Technol. 38 (10), 1125–1144.
Austad, T., RezaeiDoust, A., Puntervold, T., 2010a. Chemical Mechanism of Low Salinity Water Flooding in Sandstone Reservoirs, SPE Improved Oil Recovery Symposium. OnePetro.

Austad, T., RezaeiDoust, A., Puntervold, T., 2010b. Chemical Mechanism of Low Salinity Water Flooding in Sandstone Reservoirs. SPE Improved Oil Recovery Symposium.

Austad, T., Shariatpanahi, S.F., Strand, S., Black, C.J.J., Webb, K.J., 2012. Conditions for a low-salinity enhanced oil recovery (EOR) effect in carbonate oil reservoirs. Energy Fuel. 26 (1), 569–575.

Austad, T., Shariatpanahi, S.F., Strand, S., Aksulu, H., Puntervold, T., 2015. Low salinity EOR effects in limestone reservoir cores containing anhydrite: a discussion of the chemical mechanism. Energy Fuel. 29 (11), 6903–6911.

ХисаМов, Р., НазиМов, Н., ЕМельянов, В., Базаревская, В., Гибадуллина, О., 2020. Особенности выработки запасов углеводородного сырья из отлоЖений саргаевского горизонта на приМере скваЖин ПАО «Татнефть. Нефтяное хозяйство (7), 16–20.

Awolayo, A.N., Sarma, H.K., Nghiem, L.X., 2018. Brine-dependent recovery processes in carbonate and sandstone petroleum reservoirs: review of laboratory-field studies, interfacial mechanisms and modeling attempts. Energies 11 (11), 3020.

Ayirala, S.C., Al-Saleh, S.H., Al-Yousef, A.A., 2018a. Microscopic scale interactions of water ions at crude oil/water interface and their impact on oil mobilization in advanced water flooding. J. Petrol. Sci. Eng. 163, 640–649.

Ayirala, S.C., Yousef, A.A., Li, Z., Xu, Z., 2018b. Coalescence of crude oil droplets in brine systems: effect of individual electrolytes. Energy Fuel. 32 (5), 5763–5771.

Barnaji, M.J., Pourafshary, P., Rasaie, M.R., 2016. Visual investigation of the effects of clay minerals on enhancement of oil recovery by low salinity water flooding. Fuel 184, 826–835.

Bartels, W.-B.-B., et al., 2016. Low Salinity Flooding (LSF) in Sandstones at Pore Scale: Micro-model Development and Investigation. SPE Annual Technical Conference and Exhibition.

Bedrikovetsky, P., Zeinijahromi, A., Badalyan, A., Ahmetgareev, V., Khisamov, R., 2015. Fines-Migration-Assisted Low-Salinity Waterflooding: Field Case Analysis. SPE Russian Petroleum Technology Conference.

Bhicajee, P., Romero-Zerón, L., 2021. Effect of different low salinity flooding schemes and the addition of alkali on the performance of low-salinity waterflooding during the recovery of heavy oil from unconsolidated sandstone. Fuel 289, 119981.

Bhui, U.K., Desai, A., 2015. Swelling Study of Smectites (Montmorillonites): Implications during Low-Saline Water Flooding (LSWF) in Petroleum Reservoirs. 11th Biennial International Conference & Exposition, SPG India.

Bidhendi, M.M., Garcia-Olvera, G., Morin, B., Oakey, J.S., Alvarado, V., 2018. Interfacial viscoelasticity of crude oil/brine: an alternative enhanced-oil-recovery mechanism in smart waterflooding. SPE J. 23 (3), 803–818.

Bonto, M., Eftekhari, A.A., Nick, H.M., 2019. An overview of the oil-brine interfacial behavior and a new surface complexation model. Sci. Rep. 9 (1), 6072.

Brantson, E.T., et al., 2020a. Development of hybrid low salinity water polymer flooding numerical reservoir simulator and smart proxy model for chemical enhanced oil recovery (CEOR). J. Petrol. Sci. Eng. 187, 106751.

Brantson, E.T., et al., 2020b. Development of hybrid low salinity water polymer flooding numerical reservoir simulator and smart proxy model for chemical enhanced oil recovery (CEOR). J. Petrol. Sci. Eng. 187, 106751.

Butt, R.Z., et al., 2022. Techno-economic and environmental impact analysis of large-scale wind farms integration in weak transmission grid from mid-career repowering perspective. Sustainability 14 (5), 2507.

Cabrera S, D., Samaniego, V.F., 2022. Scaling Experimental Immiscible Flow and Geomechanics in Fractured Porous Rock, Experimental Mechanics of Fractured Porous Rocks. Springer, pp. 37–56.

Chávez-Miyauch, T.E., Lu, Y., Firoozabadi, A., 2020. Low salinity water injection in Berea sandstone: effect of wettability, interface elasticity, and acid and base functionalities. Fuel 263, 116572.

Chen, Q., Otaibi, M., Ayirala, S., Yousef, A., 2021. The prospects and potential opportunities of low salinity water flooding for offshore applications in sandstones. J. Petrol. Sci. Eng. 199, 108260.

Chen, Q., Ayirala, S., Yousef, A., 2022. A Critical Review of Low Salinity Water Flooding for Offshore Applications and Potential Opportunities. SPE Conference at Oman Petroleum & Energy Show.

Chequer, L., et al., 2019. Optimal slug size for enhanced recovery by low-salinity waterflooding due to fines migration. J. Petrol. Sci. Eng. 177, 766–785.

Chowdhury, S., Shrivastava, S., Kakati, A., Sangwai, J.S., 2022. Comprehensive review on the role of surfactants in the chemical enhanced oil recovery process. Ind. Eng. Chem. Res. 61 (1), 21–64.

Dang, C.T., Nghiem, L.X., Chen, Z., Nguyen, Q.P., 2013. Modeling Low Salinity Waterflooding: Ion Exchange, Geochemistry and Wettability Alteration. SPE Annual Technical Conference and Exhibition.

Dang, C., Nghiem, L., Nguyen, N., Chen, Z., Nguyen, Q., 2015. Modeling and Optimization of Low Salinity Waterflood. SPE Reservoir Simulation Symposium.

Dang, C., Nghiem, L., Nguyen, N., Chen, Z., Nguyen, Q., 2016a. Evaluation of CO2 low salinity water-alternating-gas for enhanced oil recovery. J. Nat. Gas Sci. Eng. 35, 237–258.

Dang, C., Nghiem, L., Nguyen, N., Chen, Z., Nguyen, Q., 2016b. Mechanistic modeling of low salinity water flooding. J. Petrol. Sci. Eng. 146, 191–209.

Darvish Sarvestani, A., Ayatollahi, S., Bahari Moghaddam, M., 2019. Smart water flooding performance in carbonate reservoirs: an experimental approach for tertiary oil recovery. J. Pet. Explor. Prod. Technol. 9 (4), 2643–2657.

Darvish Sarvestani, A., Rostami, B., Mahani, H., 2021. Polymer-enhanced low-salinity brine to control in situ mixing and salt dispersion in low-salinity waterflooding. Energy Fuel. 35 (13), 10540–10550.

Darvish Sarvestani, A., Rostami, B., Mahani, H., 2022. Impact of injection parameters on mixing control by polymer-enhanced low-salinity waterflooding. Energy Fuel. 36 (19), 11808–11816.

Deng, X., et al., 2021. Relative contribution of wettability Alteration and interfacial tension reduction in EOR: a critical review. J. Mol. Liq. 325, 115175.

Derkani, M.H., et al., 2018. Low salinity waterflooding in carbonate reservoirs: review of interfacial mechanisms. Colloids and Interfaces 2 (2), 20.

Ding, H., Wang, Y., Shapoval, A., Zhao, Y., Rahman, S., 2019. Macro- and microscopic studies of "smart water" flooding in carbonate rocks: an image-based wettability examination. Energy Fuel. 33 (8), 6961–6970.

Ding, H., Mettu, S., Rahman, S.S., 2020. Impacts of smart waters on calcite–crude oil interactions quantified by "soft tip" atomic force microscopy (AFM) and surface complexation modeling (SCM). Ind. Eng. Chem. Res. 59 (46), 20337–20348.

Dordzie, G., Dejam, M., 2021. Enhanced oil recovery from fractured carbonate reservoirs using nanoparticles with low salinity water and surfactant: a review on experimental and simulation studies. Adv. Colloid Interface Sci. 293, 102449.

Dordzie, G., Dejam, M., 2022. Experimental study on alternating injection of silica and zirconia nanoparticles with low salinity water and surfactant into fractured carbonate reservoirs for enhanced oil recovery. Ind. Eng. Chem. Res. 61 (43), 16328–16340.

Dwivedi, S., et al., 2023. Experience of Low Salinity Water Flooding in Mumbai High Field-First Offshore Field in India to Implement Enhanced Oil Recovery Technique. Offshore Technology Conference, OnePetro.

Ebaga-Ololo, J., Chon, B.H., 2018. Experimental investigation of the influence of salinity gradient on low-concentration surfactant flooding in Berea sandstone. J. Ind. Eng. Chem. 68, 355–363.

Ebrahim, T., Mohsen, V.S., Mahdi, S.M., Esmaeel, K.T., Saeb, A., 2019. Performance of low-salinity water flooding for enhanced oil recovery improved by SiO2 nanoparticles. Petrol. Sci. 16 (2), 357–365.

Emadi, A., Sohrabi, M., 2013. Visual Investigation of Oil Recovery by Low Salinity Water Injection: Formation of Water Micro-dispersions and Wettability Alteration. SPE Annual Technical Conference and Exhibition.

Fakcharoenphol, P., Kurtoglu, B., Kazemi, H., Charoenwongsa, S., Wu, Y.-S., 2014a. The effect of osmotic pressure on improve oil recovery from fractured shale formations, SPE unconventional resources conference. OnePetro.

Fakcharoenphol, P., Kurtoglu, B., Kazemi, H., Charoenwongsa, S., Wu, Y.-S., 2014b. The Effect of Osmotic Pressure on Improve Oil Recovery from Fractured Shale Formations. SPE Unconventional Resources Conference.

Fang, C., Yang, Y., Sun, S., Qiao, R., 2020. Low salinity effect on the recovery of oil trapped by nanopores: a molecular dynamics study. Fuel 261, 116443.

Farhadi, H., Fatemi, M., Ayatollahi, S., 2021. Experimental investigation on the dominating fluid-fluid and rock-fluid interactions during low salinity water flooding in water-wet and oil-wet calcites. J. Petrol. Sci. Eng. 204, 108697.

Farhadi, H., Ayatollahi, S., Fatemi, M., 2022. Impact of rock morphology on the dominating enhanced oil recovery mechanisms by low salinity water flooding in carbonate rocks. Fuel 324, 124769.

Farzaneh, S.A., et al., 2017. A Case Study of Oil Recovery Improvement by Low Salinity Water Injection. Abu Dhabi International Petroleum Exhibition & Conference.

Fathi, S.J., Austad, T., Strand, S., 2012. Water-based enhanced oil recovery EOR by smart water in carbonate reservoirs, SPE EOR conference at oil and gas west asia. OnePetro.

Fattahi Mehraban, M., Farzaneh, S.A., Sohrabi, M., Sisson, A., 2020. Novel insights into the pore-scale mechanism of low salinity water injection and the improvements on oil recovery. Energy Fuel. 34 (10), 12050–12064.

Fredriksen, S., Rognmo, A., Sandengen, K., Fernø, M., 2017a. Wettability effects on osmosis as an oil-mobilization mechanism during low-salinity waterflooding. Petrophysics 58 (1), 28–35.

Fredriksen, S.B., Rognmo, A.U., Sandengen, K., Fernø, M.A., 2017b. Wettability effects on osmosis as an oil-mobilization mechanism during low-salinity waterflooding. Petrophys. SPWLA J. Form. Eval. Reservoir Descr. 58 (1), 28–35.

Gbadamosi, A., et al., 2022. Recent advances on the application of low salinity waterflooding and chemical enhanced oil recovery. Energy Rep. 8, 9969–9996.

Ghasemi, M., Shafiei, A., 2022. Atomistic insights into role of low salinity water on montmorillonite-brine interface: implications for EOR from clay-bearing sandstone reservoirs. J. Mol. Liq. 353, 118803.

Han, S., Han, J., Kim, J.W., Lee, Y., 2022. Changes to interfacial characteristics by low salinity water/nanoparticle flooding in carbonate reservoir. J. Petrol. Sci. Eng. 208, 109711.

Hien, D., et al., 2021. Numerical simulation of low salinity water flooding on core samples for an oil reservoir in the Nam Con Son Basin. Vietnam. Energies 14 (9), 2658.

Hisham Ben, M., Shattia, A., Walid, M., 2019. Potential of low-salinity waterflooding technology to improve oil recovery. In: Ariffin, S. (Ed.), Enhanced Oil Recovery Processes. IntechOpen, Rijeka. Ch. 5.

Hossein Javadi, A., Fatemi, M., 2022. Impact of salinity on fluid/fluid and rock/fluid interactions in enhanced oil recovery by hybrid low salinity water and surfactant flooding from fractured porous media. Fuel 329, 125426.

Hussain, F., et al., 2014. Enhanced Oil Recovery through Low Salinity Fines-Assisted Waterflooding: Laboratory and Mathematical Modelling. SPE Asia Pacific Oil & Gas Conference and Exhibition.

Hussain, K.A., Chen, C., Haggerty, R., Schubert, M., Li, Y., 2022. Fundamental mechanisms and factors associated with nanoparticle-assisted enhanced oil recovery. Ind. Eng. Chem. Res. 61 (49), 17715–17734.

Jackson, M.D., Al-Mahrouqi, D., Vinogradov, J., 2016. Zeta potential in oil-water-carbonate systems and its impact on oil recovery during controlled salinity water-flooding. Sci. Rep. 6 (1), 37363.

Jadhawar, P., Saeed, M., 2023. Low salinity water and polymer flooding in sandstone reservoirs: upscaling from nano-to macro-scale using the maximum energy barrier. J. Petrol. Sci. Eng. 220, 111247.

Janssen, M.T.G., Torres Mendez, F.A., Zitha, P.L.J., 2020. Mechanistic modeling of water-alternating-gas injection and foam-assisted chemical flooding for enhanced oil recovery. Ind. Eng. Chem. Res. 59 (8), 3606–3616.
Javadi, A.H., Fatemi, M., 2022. Impact of salinity on fluid/fluid and rock/fluid interactions in enhanced oil recovery by hybrid low salinity water and surfactant flooding from fractured porous media. Fuel 329, 125426.
Jerauld, G.R., Lin, C.Y., Webb, K.J., Seccombe, J.C., 2008. Modeling low-salinity waterflooding. SPE Reservoir Eval. Eng. 11 (6), 1000–1012.
Jin, F., Du, X., Varfolomeev, M.A., Yuan, C., Du, D., 2022. Preparation and migration study of multi-walled carbon nanotube hybrid polymer gel particles: EOR implication. J. Dispersion Sci. Technol. 1–11.
Karabayanova, L., Ganiyeva, A., Pourafshary, P., Hashmet, M.R., 2022. Application of hybrid low salinity hot water flooding to enhance oil recovery from heavy oil carbonates. J. Petrol. Sci. Eng. 215, 110656.
Katende, A., Sagala, F., 2019. A critical review of low salinity water flooding: mechanism, laboratory and field application. J. Mol. Liq. 278, 627–649.
Khandoozi, S., Malayeri, M.R., Riazi, M., Ghaedi, M., 2020. Inspectional and dimensional analyses for scaling of low salinity waterflooding (LSWF): from core to field scale. J. Petrol. Sci. Eng. 189, 106956.
Kharaka, Y., Gunter, W., Aggarwal, P., Perkins, E., Debraal, J., 1988. A Computer Program for Geochemical Modeling of Water-Rock Interactions [R]. USGS Water Resources Investigation, Menlo Park, CA, USA, pp. 420–423.
Kim, Y., Kim, C., Kim, J., Kim, Y., Lee, J., 2020. Experimental investigation on the complex chemical reactions between clay minerals and brine in low salinity water-flooding. J. Ind. Eng. Chem. 89, 316–333.
Kumar, H.T., Shehata, A., Nasr-El-Din, H., 2016a. Effectiveness of Low-Salinity and CO2 Flooding Hybrid Approaches in Low-Permeability Sandstone Reservoirs. SPE Trinidad and Tobago Section Energy Resources Conference, OnePetro.
Kumar, H.T., Shehata, A.M., Nasr-El-Din, H.A., 2016b. Effectiveness of Low-Salinity and CO2 Flooding Hybrid Approaches in Low-Permeability Sandstone Reservoirs. SPE Trinidad and Tobago Section Energy Resources Conference.
Ladipo, L., Blunt, M., King, P., 2020. Optimizing low salinity waterflooding with controlled numerical influence of physical mixing considering. Uncertainty 2020 (1), 1–23.
Ladipo, L., Blunt, M.J., King, P.R., 2022. Crossflow effects on low salinity displacement in stratified heterogeneity. J. Petrol. Sci. Eng. 208, 109565.
Lager, A., Webb, K., Black, C., Singleton, M., Sorbie, K., 2006. Low Salinity Oil Recovery-An Experimental. Norway.
Lager, A., Webb, K.J., Black, C., Singleton, M., Sorbie, K.S., 2008a. Low salinity oil recovery-an experimental investigation1. Petrophys. SPWLA J. Formation Eval. Reservoir Descr. 49 (1).
Lager, A., Webb, K.J., Black, C.J.J., Singleton, M., Sorbie, K.S., 2008b. Low salinity oil recovery - an experimental Investigation1. Petrophys. SPWLA J. Form. Eval. Reservoir Descr. 49 (1).
Lager, A., Webb, K.J., Collins, I.R., Richmond, D.M., 2008c. LoSal Enhanced Oil Recovery: Evidence of Enhanced Oil Recovery at the Reservoir Scale, SPE Symposium on Improved Oil Recovery. OnePetro.
Lager, A., Webb, K.J., Collins, I.R., Richmond, D.M., 2008d. LoSal™ Enhanced Oil Recovery: Evidence of Enhanced Oil Recovery at the Reservoir Scale. SPE Symposium on Improved Oil Recovery.
Lager, A., Webb, K., Seccombe, J., 2011. Low Salinity Waterflood, Endicott, Alaska: Geochemical Study & Field Evidence of Multicomponent Ion Exchange, IOR 2011-16th European Symposium on Improved Oil Recovery. EAGE Publications BV, pp. 230–200037.
Lashkarbolooki, M., Riazi, M., Hajibagheri, F., Ayatollahi, S., 2016. Low salinity injection into asphaltenic-carbonate oil reservoir, mechanistical study. J. Mol. Liq. 216, 377–386.
Lebedeva, E., Senden, T., Knackstedt, M., Morrow, N., 2009. Improved Oil Recovery from Tensleep Sandstone–Studies of Brine-Rock Interactions by Micro-CT and AFM, IOR 2009-15th European Symposium on Improved Oil Recovery. European Association of Geoscientists & Engineers, pp. 124–100062.
Lee, K.S., Lee, J.H., 2019. Hybrid Enhanced Oil Recovery Using Smart Waterflooding. Gulf Professional Publishing.
Lee, J.H., Kim, T.H., Lee, K.S., 2018. Hybrid CO2 EOR using polymer-assisted carbonated low salinity waterflood to improve CO2 deliverability and mobility. Greenhouse Gases: Sci. Technol. 8 (3), 444–461.
Lee, J.H., Jeong, M.S., Lee, K.S., 2019a. Effects of geochemistry and interphase transport of CO2 on hybrid carbonated low salinity waterflood to improve oil recovery and CO2 sequestration. Greenhouse Gases: Sci. Technol. 9 (4), 770–788.
Lee, Y., Lee, W., Jang, Y., Sung, W., 2019b. Oil recovery by low-salinity polymer flooding in carbonate oil reservoirs. J. Petrol. Sci. Eng. 181, 106211.
Ligeiro, T.S., Vaz, A., Chequer, L., 2022. Forecasting the impact of formation damage on relative permeability during low-salinity waterflooding. J. Petrol. Sci. Eng. 208, 109500.
Ligthelm, D.J., et al., 2009. Novel Waterflooding Strategy by Manipulation of Injection Brine Composition. EUROPEC/EAGE Conference and Exhibition.
Liu, F., Wang, M., 2020. Review of low salinity waterflooding mechanisms: wettability alteration and its impact on oil recovery. Fuel 267, 117112.
Liu, Y., Block, E., Squier, J., Oakey, J., 2021. Investigating low salinity waterflooding via glass micromodels with triangular pore-throat architectures. Fuel 283, 119264.
Loahardjo, N., Xie, X., Yin, P., Morrow, N.R., 2007. Low Salinity Waterflooding of a Reservoir Rock, p. 2007. Sca.
Lyu, C., Zhong, L., Ning, Z., Chen, M., Cole, D.R., 2022. Review on underlying mechanisms of low salinity waterflooding: comparisons between sandstone and carbonate. Energy Fuel. 36 (5), 2407–2423.
Ma, S., James, L.A., 2022. Literature review of hybrid CO2 low salinity water-alternating-gas injection and investigation on hysteresis effect. Energies 15 (21), 7891.
Maaref, S., Ayatollahi, S., Rezaei, N., Masihi, M., 2017. The effect of dispersed phase salinity on water-in-oil emulsion flow performance: a micromodel study. Ind. Eng. Chem. Res. 56 (15), 4549–4561.
Mahani, H., et al., 2015. Insights into the mechanism of wettability alteration by low-salinity flooding (LSF) in carbonates. Energy Fuel. 29 (3), 1352–1367.
Mahani, H., Keya, A.L., Berg, S., Nasralla, R., 2016. Electrokinetics of carbonate/brine interface in low-salinity waterflooding: effect of brine salinity, composition, rock type, and pH on ?-Potential and a surface-complexation model. SPE J. 22 (1), 53–68.
Mahmoud, M., Elkatatny, S., Abdelgawad, K.Z., 2017. Using high- and low-salinity seawater injection to maintain the oil reservoir pressure without damage. J. Pet. Explor. Prod. Technol. 7 (2), 589–596.
Mahmoudzadeh, A., Fatemi, M., Masihi, M., 2022. Microfluidics experimental investigation of the mechanisms of enhanced oil recovery by low salinity water flooding in fractured porous media. Fuel 314, 123067.
Maki, A.W., 1992. Of measured risks: the environmental impacts of the Prudhoe Bay, Alaska, oil field. Environ. Toxicol. Chem. 11 (12), 1691–1707.
Masalmeh, S., Al-Hammadi, M., Farzaneh, A., Sohrabi, M., 2019. Low Salinity Water Flooding in Carbonate: Screening, Laboratory Quantification and Field Implementation. Abu Dhabi International Petroleum Exhibition & Conference.
McGuire, P., Chatham, J., Paskvan, F., Sommer, D., Carini, F., 2005a. Low Salinity Oil Recovery: an Exciting New EOR Opportunity for Alaska's North Slope, SPE Western Regional Meeting. OnePetro.
McGuire, P.L., Chatham, J.R., Paskvan, F.K., Sommer, D.M., Carini, F.H., 2005b. Low Salinity Oil Recovery: an Exciting New EOR Opportunity for Alaska's North Slope. SPE Western Regional Meeting.
Mehana, M., Fahes, M., Kang, Q., Viswanathan, H., 2020. Molecular simulation of double layer expansion mechanism during low-salinity waterflooding. J. Mol. Liq. 318, 114079.
Mehdizad, A., Pourafshary, P., Sedaee, B., 2022a. Visual investigation of simultaneous clay swelling and migration mechanisms and formation damage consequences using micromodels. J. Petrol. Sci. Eng. 214, 110561.
Mehdizad, A., Sedaee, B., Pourafshary, P., 2022b. Visual investigation of the effect of clay-induced fluid flow diversion on oil recovery, as a low-salinity water flooding mechanism. J. Petrol. Sci. Eng. 209, 109959.
Mehraban, M.F., Farzaneh, S.A., Sohrabi, M., Sisson, A., 2022. Fluid-fluid interactions inducing additional oil recovery during low salinity water injection in inefficacious presence of clay minerals. Fuel 308, 121922.
Miadonye, A., Irwin, D.J.G., Amadu, M., 2023. Effect of polar hydrocarbon contents on oil-water interfacial tension and implications for recent observations in smart water flooding oil recovery schemes. ACS Omega 8 (10), 9086–9100.
Mirchi, V., Saraji, S., Akbarabadi, M., Goual, L., Piri, M., 2017. A systematic study on the impact of surfactant chain length on dynamic interfacial properties in porous media: implications for enhanced oil recovery. Ind. Eng. Chem. Res. 56 (46), 13677–13695.
Mokhtari, R., Ayatollahi, S., 2019. Dissociation of polar oil components in low salinity water and its impact on crude oil–brine interfacial interactions and physical properties. Petrol. Sci. 16 (2), 328–343.
Mokhtari, R., Ayatollahi, S., Fatemi, M., 2019. Experimental investigation of the influence of fluid-fluid interactions on oil recovery during low salinity water flooding. J. Petrol. Sci. Eng. 182, 106194.
Moradpour, N., Pourafshary, P., Zivar, D., 2021. Experimental analysis of hybrid low salinity water alternating gas injection and the underlying mechanisms in carbonates. J. Petrol. Sci. Eng. 202, 108562.
Morishita, R., et al., 2020. Oil and water interactions during low-salinity enhanced oil recovery in water-wet porous media. Energy Fuel. 34 (5), 5258–5266.
Morrow, N.R., 1990. Wettability and its effect on oil recovery. J. Petrol. Technol. 42 (12), 1476–1484.
Morrow, N., Buckley, J., 2011. Improved oil recovery by low-salinity waterflooding. J. Petrol. Technol. 63 (5), 106–112.
Morrow, N.R., Tang, G.-q., Valat, M., Xie, X., 1998a. Prospects of improved oil recovery related to wettability and brine composition. J. Petrol. Sci. Eng. 20 (3–4), 267–276.
Morrow, N.R., Tang, G.-q., Valat, M., Xie, X., 1998b. Prospects of improved oil recovery related to wettability and brine composition. J. Petrol. Sci. Eng. 20 (3), 267–276.
Mukherjee, S., et al., 2020. Validation and Benchmarking of an Inorganic Aluminium-Carbamide Gel System for In-Depth and Near Wellbore Conformance Control, SPE Improved Oil Recovery Conference. OnePetro.
Mwakipunda, G.C., Ngata, M.R., Mgimba, M.M., Yu, L., 2023a. Carbon dioxide sequestration in low porosity and permeability deep saline aquifer: numerical simulation method. J. Energy Resour. Technol. 1–27.
Mwakipunda, G.C., Yang, Z., Guo, C., 2023b. Infill drilling optimization for enhanced oil recovery by waterflooding: a simulation study. J. Energy Eng. 149 (1), 04022053.
Nasralla, R.A., Nasr-El-Din, H.A., 2014. Double-layer expansion: is it a primary mechanism of improved oil recovery by low-salinity waterflooding? SPE Reservoir Eval. Eng. 17 (1), 49–59.
Nasralla, R.A., Bataweel, M.A., Nasr-El-Din, H.A., 2013. Investigation of wettability alteration and oil-recovery improvement by low-salinity water in sandstone rock. J. Can. Petrol. Technol. 52 (2), 144–154.
Nasralla, R.A., Snippe, J.R., Farajzadeh, R., 2015. Coupled Geochemical-Reservoir Model to Understand the Interaction between Low Salinity Brines and Carbonate Rock, SPE Asia Pacific Enhanced Oil Recovery Conference.
Ngata, M.R., et al., 2022a. Minireview of Formation Damage control through nanotechnology utilization at fieldwork conditions. Energy Fuel. 36 (8), 4174–4185.
Ngata, M.R., et al., 2022b. Review of developments in nanotechnology application for Formation Damage control. Energy Fuel. 36 (1), 80–97.

Nghiem, L., Sammon, P., Grabenstetter, J., Ohkuma, H., 2004. Modeling CO2 Storage in Aquifers with a Fully-Coupled Geochemical EOS Compositional Simulator. SPE/DOE Symposium on Improved Oil Recovery.
Nghiem, L., Shrivastava, V., Kohse, B., 2011. Modeling Aqueous Phase Behavior and Chemical Reactions in Compositional Simulation. SPE Reservoir Simulation Symposium.
Nguyen, N., Dang, C., Gorucu, S.E., Nghiem, L., Chen, Z., 2020. The role of fines transport in low salinity waterflooding and hybrid recovery processes. Fuel 263, 116542.
Okasha, T.M., Al-Shiwaish, A.-J.A., 2009. Effect of Brine Salinity on Interfacial Tension in Arab-D Carbonate Reservoir, Saudi Arabia, SPE Middle East Oil and Gas Show and Conference.
Olabode, O., Alaigba, D., Oramabo, D., Bamigboye, O., 2020. Modelling low-salinity water flooding as a tertiary oil recovery technique. Model. Simulat. Eng. 2020, 6485826.
Omekeh, A., Friis, H.A., Fjelde, I., Evje, S., 2012. Modeling of Ion-Exchange and Solubility in Low Salinity Water Flooding. SPE Improved Oil Recovery Symposium.
Opoku Boampong, L., Rafati, R., Sharifi Haddad, A., 2023. Modelling of carbonate rock wettability based on surface charge and calcite dissolution. Fuel 331, 125856.
Phukan, R., Saha, R., 2022. Low salinity surfactant alternating gas/CO2 flooding for enhanced oil recovery in sandstone reservoirs. J. Petrol. Sci. Eng. 212, 110253.
Piñerez Torrijos, I.D., et al., 2018. An experimental study of the low salinity Smart Water - polymer hybrid EOR effect in sandstone material. J. Petrol. Sci. Eng. 164, 219–229.
Pourafshary, P., Moradpour, N., 2019. Hybrid EOR methods utilizing low-salinity water. Enhanc. Oil Recovery Process. New Technol. 8, 25.
Pourakaberian, A., Mahani, H., Niasar, V., 2021. The impact of the electrical behavior of oil-brine-rock interfaces on the ionic transport rate in a thin film, hydrodynamic pressure, and low salinity waterflooding effect. Colloids Surf. A Physicochem. Eng. Asp. 620, 126543.
Pourakaberian, A., Mahani, H., Niasar, V., 2022. Dynamics of electrostatic interaction and electrodiffusion in a charged thin film with nanoscale physicochemical heterogeneity: implications for low-salinity waterflooding. Colloids Surf. A Physicochem. Eng. Asp. 650, 129514.
Pouryousefy, E., Xie, Q., Saeedi, A., 2016. Effect of multi-component ions exchange on low salinity EOR: coupled geochemical simulation study. Petroleum 2 (3), 215–224.
Pu, H., Xie, X., Yin, P., Morrow, N., 2008. Application of Coalbed Methane Water to Oil Recovery by Low Salinity Waterflooding. Paper SPE 113410 presented at the SPE, DOE Symposium on Improved Oil Recovery, Tulsa, Oklahoma, pp. 20–23.
Pu, H., Xie, X., Yin, P., Morrow, N.R., 2010. Low Salinity Waterflooding and Mineral Dissolution. SPE Annual Technical Conference and Exhibition.
Qiao, C., Johns, R., Li, L., 2016. Modeling low-salinity waterflooding in chalk and limestone reservoirs. Energy Fuel. 30 (2), 884–895.
Rahevar, S., et al., 2023. Controlled salinity water flooding and zeta potential: insight into a novel enhanced oil recovery mechanism. Energy Rep. 9, 2557–2565.
Ramanathan, R., Shehata, A.M., Nasr-El-Din, H.A., 2016. Effect of Rock Aging on Oil Recovery during Water-Alternating-CO2 Injection Process: an Interfacial Tension, Contact Angle, Coreflood, and CT Scan Study. SPE Improved Oil Recovery Conference.
RezaeiDoust, A., Puntervold, T., Strand, S., Austad, T., 2009. Smart water as wettability modifier in carbonate and sandstone: a discussion of similarities/differences in the chemical mechanisms. Energy Fuel. 23 (9), 4479–4485.
Ridwan, M.G., et al., 2020. Low salinity waterflooding: surface roughening and pore size alteration implications. J. Petrol. Sci. Eng. 195, 107868.
Robbana, E., et al., 2012. Low Salinity Enhanced Oil Recovery - Laboratory to Day One Field Implementation - LoSal EOR into the Clair Ridge Project. Abu Dhabi International Petroleum Conference and Exhibition.
Rotondi, M., Callegaro, C., Masserano, F., Bartosek, M., 2014a. Low salinity water injection: eni's experience, Abu Dhabi international petroleum exhibition and conference. OnePetro.
Rotondi, M., Callegaro, C., Masserano, F., Bartosek, M., 2014b. Low Salinity Water Injection: Eni's Experience, Abu Dhabi International Petroleum Exhibition and Conference.
Sagala, F., Hethnawi, A., Nassar, N.N., 2020. Integrating silicate-based nanoparticles with low-salinity water flooding for enhanced oil recovery in sandstone reservoirs. Ind. Eng. Chem. Res. 59 (37), 16225–16239.
Sagbana, P.I., Sarkodie, K., Nkrumah, W.A., 2022. A Critical Review of Carbonate Reservoir Wettability Modification during Low Salinity Waterflooding. Petroleum.
Samanova, A., 2021. Surfactant/LSW Flooding in Carbonates: an Investigation of Hybrid EOR Method Design to Improve Oil Displacement.
Sami, B., Azdarpour, A., Honarvar, B., Nabipour, M., Keshavarz, A., 2022. Application of a novel natural surfactant extracted from Avena Sativa for enhanced oil recovery during low salinity water flooding: synergism of natural surfactant with different salts. J. Mol. Liq. 362, 119693.
Samsuri, A., 2019. Enhanced Oil Recovery Processes: New Technologies. BoD–Books on Demand.
Sandengen, K., Arntzen, O., 2013. Osmosis during Low Salinity Water Flooding, IOR 2013-17th European Symposium on Improved Oil Recovery. European Association of Geoscientists & Engineers, pp. 342–300015.
Sandengen, K., Kristoffersen, A., Melhuus, K., Jøsang, L.O., 2016. Osmosis as mechanism for low-salinity enhanced oil recovery. SPE J. 21 (4), 1227–1235.
Saw, R.K., Mandal, A., 2020. A mechanistic investigation of low salinity water flooding coupled with ion tuning for enhanced oil recovery. RSC Adv. 10 (69), 42570–42583.
Saw, R.K., Pillai, P., Mandal, A., 2022. Synergistic effect of low saline ion tuned Sea Water with ionic liquids for enhanced oil recovery from carbonate reservoirs. J. Mol. Liq. 364, 120011.
Schembre, J.M., Kovscek, A.R., 2005. Mechanism of Formation Damage at elevated temperature. J. Energy Resour. Technol. 127 (3), 171–180.
Seccombe, J.C., Lager, A., Webb, K., Jerauld, G., Fueg, E., 2008. Improving Wateflood Recovery: LoSal™ EOR Field Evaluation. SPE Symposium on Improved Oil Recovery.
Seccombe, J., et al., 2010. Demonstration of Low-Salinity EOR at Interwell Scale, Endicott Field, Alaska, SPE Improved Oil Recovery Symposium. OnePetro.
Shabani, A., Zivar, D., 2020. Detailed analysis of the brine-rock interactions during low salinity water injection by a coupled geochemical-transport model. Chem. Geol. 537, 119484.
Shabib-Asl, A., Ayoub, M.A., Elraies, K.A., 2019. A new hybrid technique using low salinity water injection and foam flooding for enhanced oil recovery in sandstone rock. J. Petrol. Sci. Eng. 174, 716–728.
Shafiei, A., Tatar, A., Rayhani, M., Kairat, M., Askarova, I., 2022. Artificial neural network, support vector machine, decision tree, random forest, and committee machine intelligent system help to improve performance prediction of low salinity water injection in carbonate oil reservoirs. J. Petrol. Sci. Eng. 219, 111046.
Shakeel, M., Samanova, A., Pourafshary, P., Hashmet, M.R., 2022. Optimization of low salinity water/surfactant flooding design for oil-wet carbonate reservoirs by introducing a negative salinity gradient. Energies 15 (24), 9400.
Sharma, M., Filoco, P., 2000. Effect of brine salinity and crude-oil properties on oil recovery and residual saturations. SPE J. 5 (3), 293–300.
Sharma, H., Mohanty, K.K., 2018. An experimental and modeling study to investigate brine-rock interactions during low salinity water flooding in carbonates. J. Petrol. Sci. Eng. 165, 1021–1039.
Shehata, A.M., Nasr-El-Din, H.A., 2015. Zeta Potential Measurements: Impact of Salinity on Sandstone Minerals. SPE International Symposium on Oilfield Chemistry. OnePetro.
Sheng, J.J., 2014. Critical review of low-salinity waterflooding. J. Petrol. Sci. Eng. 120, 216–224.
Shi, H., Liu, Y., He, Y., Xu, W., 2021. The Simulation and Pilot Application of Low Salinity Water Flooding for Offshore Low Permeability Reservoir, International Petroleum Technology Conference. OnePetro.
Shojaei, M.-J., Ghazanfari, M.H., Masihi, M., 2015. Relative permeability and capillary pressure curves for low salinity water flooding in sandstone rocks. J. Nat. Gas Sci. Eng. 25, 30–38.
Siadatifar, S.E., Fatemi, M., Masihi, M., 2021. Pore scale visualization of fluid-fluid and rock-fluid interactions during low-salinity waterflooding in carbonate and sandstone representing micromodels. J. Petrol. Sci. Eng. 198, 108156.
Skrettingland, K., Holt, T., Tweheyo, M.T.T., Skjevrak, I., 2011. Snorre low-salinity-water injection—coreflooding experiments and single-well field pilot. SPE Reservoir Eval. Eng. 14 (2), 182–192.
Skrettingland, K., et al., 2016. Snorre In-Depth Water Diversion - New Operational Concept for Large Scale Chemical Injection from a Shuttle Tanker. SPE Improved Oil Recovery Conference.
Sohal, M.A., Kucheryavskiy, S., Thyne, G., Søgaard, E.G., 2017. Study of ionically modified water performance in the carbonate reservoir system by multivariate data analysis. Energy Fuel. 31 (3), 2414–2429.
Song, W., Kovscek, A.R., 2016. Direct visualization of pore-scale fines migration and formation damage during low-salinity waterflooding. J. Nat. Gas Sci. Eng. 34, 1276–1283.
Takeda, M., Manaka, M., Tuji, T., 2021. Chemical osmosis as a cause for the improved oil recovery by low-salinity water flooding: experimental and numerical approaches for detection. J. Petrol. Sci. Eng. 207, 109090.
Takeya, M., Shimokawara, M., Elakneswaran, Y., Nawa, T., Takahashi, S., 2019. Predicting the electrokinetic properties of the crude oil/brine interface for enhanced oil recovery in low salinity water flooding. Fuel 235, 822–831.
Taleb, M., Sagala, F., Hethnawi, A., Nassar, N.N., 2021. Enhanced oil recovery from austin chalk carbonate reservoirs using faujasite-based nanoparticles combined with low-salinity water flooding. Energy Fuel. 35 (1), 213–225.
Tang, G.-Q., Morrow, N.R., 1999a. Influence of brine composition and fines migration on crude oil/brine/rock interactions and oil recovery. J. Petrol. Sci. Eng. 24 (2), 99–111.
Tang, G.-Q., Morrow, N.R., 1999b. Influence of brine composition and fines migration on crude oil/brine/rock interactions and oil recovery. J. Petrol. Sci. Eng. 24 (2–4), 99–111.
Tatar, A., Askarova, I., Shafiei, A., Rayhani, M., 2021. Data-driven connectionist models for performance prediction of low salinity waterflooding in sandstone reservoirs. ACS Omega 6 (47), 32304–32326.
Teklu, T.W., 2015. Experimental and Numerical Study of Carbon Dioxide Injection Enhanced Oil Recovery in Low-Permeability Reservoirs. Colorado School of Mines. Arthur Lakes Library.
Teklu, T.W., Alameri, W., Kazemi, H., Graves, R.M., AlSumaiti, A.M., 2017. Low salinity water–Surfactant–CO2 EOR. Petroleum 3 (3), 309–320.
Tetteh, J.T., Barati, R., 2018. Crude-oil/brine interaction as a recovery mechanism for low-salinity waterflooding of carbonate reservoirs. SPE Reservoir Eval. Eng. 22 (3), 877–896.
Torrijos, I.D.P., et al., 2018. An experimental study of the low salinity Smart Water-Polymer hybrid EOR effect in sandstone material. J. Petrol. Sci. Eng. 164, 219–229.
Tripathi, I., Mohanty, K.K., 2008. Instability due to wettability alteration in displacements through porous media. Chem. Eng. Sci. 63 (21), 5366–5374.
Vledder, P., Fonseca, J.C., Wells, T., Gonzalez, I., Ligthelm, D., 2010. Low Salinity Water Flooding: Proof of Wettability Alteration on a Field Wide Scale. SPE Improved Oil Recovery Symposium. OnePetro.
Webb, K., Black, C.a., Al-Ajeel, H., 2004. Low Salinity Oil Recovery-Log-Inject-Log. SPE/DOE Symposium on Improved Oil Recovery, OnePetro.

Webb, K.J., Black, C.J.J., Tjetland, G., 2005. A Laboratory Study Investigating Methods for Improving Oil Recovery in Carbonates, International Petroleum Technology Conference.
Willhite, G.P., 1986. Waterflooding.
Wilson, A., 2014. UK field benefits from reduced-salinity enhanced-oil-recovery implementation. J. Petrol. Technol. 66 (1), 66–68.
Winoto, W., Loahardjo, N., Xie, X.S., Yin, P., Morrow, N.R., 2012. Secondary and Tertiary Recovery of Crude Oil from Outcrop and Reservoir Rocks by Low Salinity Waterflooding, SPE Improved Oil Recovery Symposium. OnePetro.
Woidneck, K., Behrman, P., Soule, C., Wu, J., 1987. Reservoir Description of the Endicott Field (North Slope, Alaska).
Wood, D.A., Yuan, B., 2018. Low-Salinity Water Flooding: from Novel to Mature Technology, Formation Damage during Improved Oil Recovery. Elsevier, pp. 21–67.
Wood, A., Wilcox, T., MacDonald, D., Flynn, J., Angert, P., 1991. Determining Effective Residual Oil Saturation for Mixed Wettability Reservoirs: Endicott Field, Alaska. SPE Annual Technical Conference and Exhibition, OnePetro.
Xiao, R., Gupta, R., Glotzbach, R.C., Sinha, S., Teletzke, G.F., 2018. Evaluation of low-salinity waterflooding in Middle East carbonate reservoirs using a novel, field-representative coreflood method. J. Petrol. Sci. Eng. 163, 683–690.
Xie, Q., et al., 2019. Effect of electrical double layer and ion exchange on low salinity EOR in a pH controlled system. J. Petrol. Sci. Eng. 174, 418–424.
Yan, L., Aslannejad, H., Hassanizadeh, S.M., Raoof, A., 2020. Impact of water salinity differential on a crude oil droplet constrained in a capillary: pore-scale mechanisms. Fuel 274, 117798.
Yousef, A.A., Al-Saleh, S., Al-Kaabi, A., Al-Jawfi, M., 2011. Laboratory investigation of the impact of injection-water salinity and ionic content on oil recovery from carbonate reservoirs. SPE Reservoir Eval. Eng. 14 (5), 578–593.
Yousef, A.A., Al-Saleh, S., Al-Jawfi, M., 2012. Improved/Enhanced Oil Recovery from Carbonate Reservoirs by Tuning Injection Water Salinity and Ionic Content. SPE Improved Oil Recovery Symposium.
Yu, M., et al., 2018. Imaging analysis of fines migration during water flow with salinity alteration. Adv. Water Resour. 121, 150–161.
Yu, M., et al., 2019. Effects of fines migration on oil displacement by low-salinity water. J. Petrol. Sci. Eng. 175, 665–680.
Yuan, B., Moghanloo, R.G., 2018. Nanofluid pre-treatment, an effective strategy to improve the performance of low-salinity waterflooding. J. Petrol. Sci. Eng. 165, 978–991.
Yutkin, M.P., Radke, C.J., Patzek, T.W., 2022. Chemical compositions in modified salinity waterflooding of calcium carbonate reservoirs: experiment. Transport Porous Media 141 (2), 255–278.
Zeinijahromi, A., Lemon, P.E., Bedrikovetsky, P., 2011. Effects of induced fines migration on water cut during waterflooding. J. Petrol. Sci. Eng. 78, 609–617.
Zeinijahromi, A., Al-Jassasi, H., Begg, S., Bedrikovetski, P., 2015. Improving sweep efficiency of edge-water drive reservoirs using induced formation damage. J. Petrol. Sci. Eng. 130, 123–129.
Zeinijahromi, A., Farajzadeh, R., Bruining, J., Bedrikovetsky, P., 2016. Effect of fines migration on oil–water relative permeability during two-phase flow in porous media. Fuel 176, 222–236.
Zhang, Y., Morrow, N.R., 2006. Comparison of secondary and tertiary recovery with change in injection brine composition for crude-oil/sandstone combinations, SPE/DOE symposium on improved oil recovery. OnePetro.
Zhang, Y., Sarma, H., 2012. Improving Waterflood Recovery Efficiency in Carbonate Reservoirs through Salinity Variations and Ionic Exchanges: A Promising Low-Cost. Smart-Waterflood" Approach, Abu Dhabi International Petroleum Conference and Exhibition.
Zhang, Y., Xie, X., Morrow, N.R., 2007. Waterflood performance by injection of brine with different salinity for reservoir cores, SPE annual technical conference and exhibition. OnePetro.